Energy & Environmental Science

ROYAL SOCIETY OF CHEMISTRY

PAPER

View Article Online
View Journal | View Issue

Cite this: *Energy Environ. Sci.*, 2024, **17**, 1931

Green ethylene production in the UK by 2035: a techno-economic assessment†

Andreas H. Nyhus,‡ Maria Yliruka,*‡ Nilay Shah and Benoît Chachuat*

Olefins production in the UK is the most emission-intensive sector of the chemical industry. Bringing thermocatalytic and electrocatalytic processes together, this paper compares nine process routes for green ethylene production from air-captured CO_2 and off-shore wind electricity in order to displace fossil-based ethylene, with a particular focus on technology readiness for near-future deployment. The methanol-mediated thermocatalytic route has the lowest projected levelised cost at £2900 per ton of ethylene by 2035, closely followed by direct and tandem CO_2 electroreduction routes in the range £2900–3200. The price of green ethylene at three times or more its current market price is confirmed through a sensitivity analysis varying the levelised cost of electricity, stack cost, and market price of propylene or oxygen simultaneously. While these green ethylene production processes would be carbon negative from a cradle-to-gate viewpoint, displacing a conventional ethane cracker with annual production capacity of 800 kt could consume as much as 46–66 TW h of renewable electricity, which is a major barrier to deployment.

Received 12th September 2023,
Accepted 17th January 2024

DOI: 10.1039/d3ee03064d

rsc.li/ees

Broader context

Ethylene is the most widely produced organic compound globally. For decades, steam cracking has been the dominant method to produce ethylene from fossil fuels but its production is one of the largest CO_2-emitting processes in the chemical industry, calling for the development of more sustainable production routes. Of the alternatives to defossilise ethylene, is the use of CO_2 captured from ambient air as feedstock and renewable electricity from offshore wind in order for the produced ethylene to be fully compliant with the green chemical standard. Candidate technologies for producing such green ethylene at scale include a range of conventional and unconventional, thermocatalytic and electrocatalytic processes, which have to date been assessed separately and often using process boundaries that fail to comply with the green production standard. The techno-economic assessment here fills in this gap and seeks to predict a lower bound on future market price of green ethylene by 2035, with a particular focus on the UK context.

1 Introduction

Light olefins, comprising ethylene and propylene, are fundamental building blocks in the chemical industry for the production of plastics, synthetic fibers and synthetic rubbers.[1,2] In Europe light olefins are mostly produced through naphtha steam-cracking, while in the United Kingdom (UK) and the United States (US) alkane steam crackers are more common.[3–5] A typical ethane cracker produces about 50% ethylene, 35% ethane, 5% C_{3+}, and additional light hydrocarbons.[2] In the UK alone, the annual olefins production amounts to 2.75 Mt and emits 3.1 Mt of CO_2, making it the most emission-intensive process across the UK's chemical sector (share of 17%).[6,7] It contributed about 0.5% of the UK's total greenhouse gas (GHG) emissions in 2019.[8,9] Defossilising olefins production is particularly challenging given that fossil fuels are not only used to meet the utility demands, but also as the carbon feedstock itself.[10]

Biomass, polymers and CO_2 are all candidate feedstocks for defossilising light olefins and olefin-derived products.[11–17] Since sustainably-sourced lignocellulosic biomass is in limited supply, its use may rather be prioritised for negative emission technologies such as bioenergy for power plants coupled with carbon capture and long-term geological storage.[18] Challenges with polymer recycling, either mechanically or chemically, arise due to feedstock heterogeneity and availability.[19] The number of times a polymer can undergo mechanical recycling is furthermore limited due to the degradation of its mechanical properties,[20] while additives and impurities can cause catalyst deactivation in chemical recycling processes.[21,22] In contrast to

The Sargent Centre for Process Systems Engineering, Department of Chemical Engineering, Imperial College London, Exhibition Road, London, SW7 2AZ, UK. E-mail: m.yliruka@imperial.ac.uk, b.chachuat@imperial.ac.uk

† Electronic supplementary information (ESI) available. See DOI: https://doi.org/10.1039/d3ee03064d

‡ These authors contributed equally to this work.

biomass and plastic waste, CO_2 captured from industrial processes or extracted from the atmosphere can be purified to meet process specification for its utilisation. The UK has large CO_2 storage capacities and aims to become a global leader in carbon capture, utilisation, and storage.[23] The industrial clusters around Merseyside and on the East coast are expected to capture, respectively, 10 and 27 Mt_{CO_2} annually from industrial point sources from 2030.[24–26] Large quantities of CO_2 could therefore become available for CO_2 utilisation projects, although no such development is yet planned in the UK.[27] While CO_2 from industrial processes and power plants remains ultimately linked to fossil fuel consumption, direct air capture (DAC) already has a negative carbon footprint for the current UK electricity mix (0.18 kg_{CO_2} kW h^{-1} in 2022).[28,29] Following the terminology applied to hydrogen production processes,[30] only a production route based on atmospheric carbon and renewable energy may indeed qualify as green.

Two pathways for the utilisation of CO_2 using renewable energy include: (i) thermocatalytic processes reliant on green hydrogen, and (ii) electroreduction of CO_2 (CO_2RR) powered by renewable electricity. The former can benefit from the economy of scale for large production volumes, minimize utility demands *via* heat integration, and produce valuable hydrocarbon co-products. Although at a lower technology readiness level (TRL) than thermocatalytic processes, CO_2RR avoids losses incurred in converting electricity to hydrogen and will benefit from the large technological learning rates projected for hydrogen electrolysers in the near future (*e.g.*, from \$880 kW^{-1} today down to \$400 kW^{-1} by 2030 for 10 MW PEM electrolysers).[31] CO_2RR may be used to directly produce ethylene or alternatively produce an intermediate that is subsequently converted to ethylene. Nevertheless, low-margins force the chemical industry to be risk-averse, causing a preference for thermocatalytic technologies which have greater maturity.[32] Additionally, the delay induced by waiting for a low-TRL technology to become mature comes at the risk of missing emission reduction targets.[33] There is a need, therefore, for comparing the available routes from CO_2 and renewable energy to ethylene in a systematic manner, through taking current performance into account to decide whether to prioritise investment into scale-up or further research-and-development. Investment into the defossilisation of ethylene would have a significant impact across the chemical sector, as its embedded emissions are currently a major contributor to the cradle-to-gate emissions of numerous downstream products, including low- and high-density polyethylene (LDPE, HDPE), polyethylene terephthalate (PET), and polyvinyl chloride (PVC).[34,35]

1.1 Techno-economic review

Multiple techno-economic assessments of CO_2 electroreduction processes have set out to determine which products could become competitive with conventional production routes, most commonly, formic acid, ethanol, carbon monoxide and ethylene.[36–39] Orella *et al.*[37] further included methane, Verma *et al.*[38] methanol, and Jouny *et al.*[39] methanol and *n*-propanol. Having the highest product value per electron, formic acid and carbon monoxide were the only products with positive end-of-life net present values under current market prices. Ethylene produced *via* CO_2RR could be competitive with naphtha cracking, although not with ethane cracking.[36] None of these studies focused on green ethylene production but instead assumed processes powered with grid electricity in a price range of \$30–60 MW h^{-1} and fed with CO_2 captured from large point sources at a price of \$16.5–70 $t_{CO_2}^{-1}$ to minimise production cost. Disregarding the alkaline conditions commonly used in CO_2RR experiments, idealised assumptions were made for CO_2 electrolysers with proton-exchange membrane (PEM) in terms of their faradaic efficiency, current density, and single-pass conversion. Additionally, liquid and gas separation costs were taken proportional to the product flowrates rather than based on the actual product composition.

Going beyond the CO_2 electroreduction processes, existing comparisons between thermocatalytic and electrocatalytic processes for producing methanol,[40,41] methane[42] and syngas[43] from CO_2 concluded that the former would be more profitable. It was also found that the production cost of these chemicals is typically driven by operating costs, accounting for more than 60% of the total cost. The losses incurred in the conversion of renewable electricity to H_2 in any of the thermocatalytic routes could be afforded because water electrolysers presently enjoy higher energy efficiencies (around 70%) than CO_2 electrolysers (dependent on target product but typically below 50%).[40,42,43] A limitation in all of these studies is that the levelised cost of renewable electricity was set equal to the price of electricity, thereby neglecting the cost of balancing both daily and seasonal intermittency. Kim *et al.*[41] even assumed a plant operation using free, surplus renewable electricity. Again, idealised assumptions on the performance of CO_2 electrolysers were made,[40,41] and only Welch *et al.*[42] and Moreno-Gonzalez *et al.*[43] considered a CO_2 feedstock from DAC, which is necessary for the produced chemicals to qualify as green.

Regarding the complete route from CO_2 to ethylene using renewable electricity, the thermocatalytic conversion of CO_2 to methanol then to olefins (MS+MTO) was compared to CO_2 methanation followed by oxidative coupling of methane (CTM+OCM)[44] and to direct Fischer–Tropsch synthesis from CO_2 (D-FT).[45] Based on the energy content of the products, ethylene from D-FT could cost eight times as much as from MS+MTO due to the large utility requirement for the compression and pre-heating of its recycle stream. Ethylene from CTM+OCM could also be twice as costly as from MS+MTO,[44] although the corresponding assessment did not account for differences in the product stream composition. In separate comparisons,[46,47] both the MS and MTO stages were found to be cheaper than CTM and OCM, respectively. The cost advantage of MS over CTM was driven by the lower $H_2:CO_2$ ratio while MTO outcompeted OCM by generating a larger revenue from selling propylene compared to ethylene in the US market. Focusing only on electrocatalytic processes, Ramdin *et al.*[48] compared the direct CO_2RR to ethylene (D-eC_2H_4) to a two-stage electrolysis process converting CO_2 to CO either at high- or low-temperature, followed by CO electroreduction (CORR) to ethylene. The high-

temperature two-step route was predicted to be cheaper, while the total cost of both low-temperature routes were comparable. Modelling the separation processes in more detail than other studies, Ramdin *et al.*[48] also confirmed the dominant costs to be the capital and operating costs of the electrolysers, contributing over 75% of the total system cost. Bringing together both types of processes, Ioannou *et al.*[49] compared the electrocatalytic D-eC_2H_4 route to the thermocatalytic MS+MTO route. The latter was found to be the cheaper alternative since it had lower capital costs and could benefit from the higher energy efficiency of H_2 electrolysers (65%) compared to CO_2 electrolysers (34%). For scenarios in which electricity was generated by nuclear reactors or onshore wind turbines, Ioannou *et al.*[49] predicted negative global warming potentials for both routes, yet production costs two to three times larger than naphtha cracking.

1.2 Contributions and outline

The techno-economic review above identifies the methanol-mediated thermocatalytic route as a promising candidate for low-cost green ethylene production from CO_2 and renewable energy. While combined electrocatalytic and thermocatalytic processes *via* syngas and methanol have been reviewed,[50] none of these combinations have been systematically compared through techno-economic analysis. Disparate system boundaries and costing methodologies in existing, often pairwise assessments make it difficult to draw meaningful conclusions about their overall cost-competitiveness.

To supply either CO_2 utilisation pathway with green electricity and hydrogen, the UK's renewable power generation capacity would need to be expanded.[51] A whole systems perspective is much needed to account for the limitations on renewable generation capacity due to land availability, cost and public acceptance.[51] However, current scenarios for the UK's future energy system fail to reflect these additional demands,[52–54] due in part to the difficulty of integrating chemical production processes into whole-system energy modelling. Deciding early on a decarbonisation strategy across different sectors is however paramount to reducing the overall system costs associated with the transition to net-zero by 2050.[55]

This paper presents a comprehensive techno-economic analysis of nine process routes for green ethylene production from air-captured CO_2 and renewable electricity from a dedicated offshore wind farm, by bringing thermocatalytic and electrocatalytic processes together. Using consistent system boundaries, process inventories are derived from best-in-class, heat-integrated thermocatalytic processes and both low- and high-temperature CO_2 or CO electrolysers. The candidate routes are ranked according to the levelised cost of ethylene and a sensitivity analysis is conducted to confirm that the conclusions are robust towards changes in the levelised cost of electricity, stack cost, and market price of co-products. While the focus of this work lies in the comparison of defossilised ethylene production pathways on a process level, the process inventories computed herein could be used as part of any energy system model too.

The rest of the paper is structured as follows: Section 2 starts with reviewing the technology readiness and process conditions for selected production routes to green ethylene, then details the process modelling and levelised cost calculation methodology. Section 3 discusses the predicted process inventories and levelised costs of ethylene production for each route, before analysing the sensitivity of the top two routes, and examining systemic consequences beyond the process boundaries. Finally, Section 4 concludes the paper.

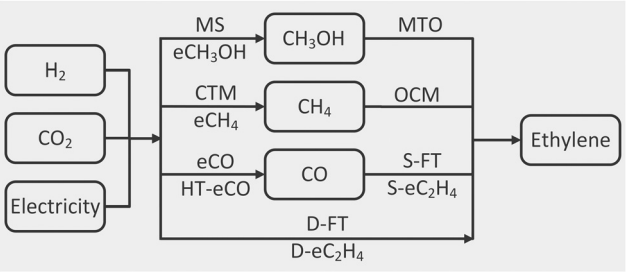

Fig. 1 Overview of the processes and intermediates in the conversion of CO_2 to ethylene. Abbreviations: MS: methanol synthesis; eCH_3OH: CO_2 electroreduction to methanol; MTO: methanol to olefin; CTM: CO_2 methanation; eCH_4: CO_2 electroreduction to methane; OCM: oxidative coupling of methane; eCO: CO_2 electroreduction to CO; HT-eCO: high-temperature CO_2 electroreduction to CO; S-FT: syngas Fischer–Tropsch; S-eC_2H_4: CO electroreduction to ethylene; D-FT: direct Fischer–Tropsch; D-eC_2H_4: CO_2 electroreduction to ethylene. Refer to Section A of the Appendix for details.

2 Methodology

2.1 Technology selection and modelling

A common system boundary is set around each process so that only renewable electricity, green hydrogen, CO_2, air and water can enter, while only ethylene, hydrocarbon co-products, oxygen, residual CO_2 and wastewater can leave. All hydrocarbon mixtures are separated in terms of their ethylene, ethane, propylene, propane, methane or C_{4+} constituents. Residual emissions from purge streams and carbon-capture processes and wastewater from the separation and purification are also accounted for as outputs.

The processes of interest (Fig. 1) convert CO_2 into ethylene either directly or *via* a single one-carbon intermediate (CO, CH_4 and CH_3OH). The conversion of CO_2 to an intermediate is referred to as stage-1 and the subsequent conversion of the intermediate to ethylene as stage-2. For those processes needing syngas in stage-2, *in situ* produced CO is combined with green H_2 in the relevant stoichiometry ratio. The ethylene production rate from stage-2 governs the production rate of the intermediate from stage-1, and both stages are integrated. Any unconverted CO_2 or H_2 from stage-2 is recycled to stage-1. Similarly, the heat and electricity utility demands of one stage may be met by excess heat or electricity from the other stage. A more systematic process integration using optimisation was beyond the scope of this work.

A key outcome of the modelling conducted herein is linear input-output models for each (single- or two-stage) process derived from the detailed mass and energy process inventories

and normalised to the production of 1 tonne of ethylene in the manner of a functional unit in life-cycle assessment (LCA). Such linear models are particularly suitable for integration into energy system models as part of future research.

2.1.1 Thermocatalytic processes. Three criteria were applied for the selection of thermocatalytic process models: first, a reactor model should be based on reaction kinetics to reflect realistic performance levels, with preference given to commercial processes where available. Second, a process should be heat-integrated in order to minimise utility requirements and reflect the true potential of thermocatalytic processes. Third, the flowsheet, mass and energy balances, and cost analysis should be explicitly modelled to enable rescaling of all the relevant units under a common system boundary.

The reference process are adapted to the new system boundary for green ethylene production by excluding any process unit generating an intermediate from fossil resources and including an air separation unit where a pure oxygen feed stream is required.[56] Where applicable, the cryogenic distillation train by Liu *et al.*[57] is added for the separation of hydrocarbon mixtures.

The mass and energy balances are subsequently updated, including the recycling of concentrated CO_2 and H_2 streams and any purge and flue gas streams. The utility demands are met by first integrating any excess heat and electricity. Where a net heat surplus is available after integration, a condensing steam turbine is designed to produce electricity.[58] And where a net import of hot utility is required, the system is extended to include a hydrogen boiler. Finally, capital expenses from the reference processes are scaled according to the six-tenth rule[58] and converted to 2019 prices using the Chemical Engineering Plant Cost Index (CEPCI).[59]

Refer to Section A of the appendix and Section S1 of the ESI,† for further details about the reference processes, including any adjustments made.

2.1.2 Low-temperature electrocatalytic processes. Although low-temperature CO_2 and CO electrolysers have improved tremendously over the last decade, their technological maturity remains low (TRL 4). The screening of electrocatalytic processes therefore focuses on state-of-the-art lab-scale performance with preference given to: common cathode material, membrane type and electrolyte; flow cell experimental set-ups over H-cell configurations;[60] and experimental studies showing sustained performance for longer than 1 hour. Where several such studies can be found, the final choice is based on the highest current density (to reduce the capital cost) and lowest cell voltage (to reduce the electricity demand).[39]

The electrochemical model describes the relationship between the electrical power and CO_2 (or CO) feed rate with the flow rate of product. The electric current is set by the flow rate and the faradaic efficiency (η_F) of the product, while the required electrode area (A_{cell}) follows from the current density (j). The cell voltage (E_{cell}) is calculated based on the half-cell potentials of the CO_2RR (E_{red}) and oxygen evolution reaction (OER), which depart from the standard cell potentials due to both activation potentials and ohmic losses. While the half-cell potential at the anode could be reduced by oxidising organic molecules instead of water,[61,62] this option would not be compliant with the set system boundary around renewable electricity, H_2, CO_2, air and water (*cf.* Section 2.1). The flow rates of the co-products and reactants are estimated from the product flow rate, the electrochemical reaction's stoichiometry (*cf.* Section A of the Appendix) and the single-pass CO_2 or CO conversion (X). The parameter values for the electrocatalytic processes of interest are summarised in Table 1. The faradaic efficiencies, current densities, and cell voltages were all measured experimentally. The set single-pass CO_2 or CO conversions of 40% were not measured, but deemed achievable by 2035 based on 10–40% conversion values reported in recent alkaline zero-gap electrolysers,[63–66] largely limited by carbon losses due to carbonate formation.[67,68]

Table 1 Parameters used in the electrochemical model of each reference process. Refer to Appendix A for details about the reference processes and to Section S2.1.1 of the ESI for cell voltage calculations

		Parameters				
Process	Ref.	η_F (—)	X (—)	j (A m^{-2})	E_{red} (V)	E_{cell} (V)
eCO	69	1.00	0.40	3500	1.63	2.83
eCH_4	70	0.73	0.40	5000	2.31	3.51
S-eC_2H_4	71	0.69	0.40	1500	1.61	2.81
D-eC_2H_4	72	0.66	0.40	1100	1.43	2.63

For the scale up of CO_2 and CO electrolysers, a zero-gap cell design is preferred to a flow cell design as it reduces the overall cell resistance and increases performance, particularly at high current densities.[66,73] The cell design and the balance of plant (BOP) layout of anion-exchange membrane (AEM) electrolysers are analogous to those of PEM electrolysers.[74] A similar expression therefore is used for their capital cost, building on a specific stack cost estimate around £280 kW^{-1} by 2035.[75] For 1 MW PEM electrolysers, the stack cost contributes about 35% of the total system cost;[76] the BOP makes the other 65% in terms of power supply, deionised water circulation system, gas processing and cooling equipment, all expected to be manufactured at scale for electrolyer systems by 2035. Whereas the cost of the BOP scales with the power consumption of the electrolyser, the stack cost correlates with the electrode area.

To separate ethylene from the mixed gas products of the electrolysers, vacuum pressure swing adsorption (VPSA) processes are used,[48,77] and any unconverted CO_2 is recovered and recycled at a 97% capture rate by mixed-amine CO_2 absorption.[78] The separation of the liquid co-products (acetic acid, alcohols) is also considered when their concentration in the electrolyte exceeds 20 wt%. The utility demands of the separation train are met by hydrogen boilers and renewable electricity imports because they cannot be heat-integrated with the low-temperature electrolysers. Both the capital and utility costs of the separation processes are scaled up according to the total product flow rate. The total invested capital (TIC) comprises the fixed capital investments for the CO_2 electrolyser and its associated separation train, as well as additional working capital, start-up and contingency costs.[79]

Refer to Section A of the Appendix for additional details about the reference CO_2 electrolysers and to Section S2 of the ESI,† for further details about the electrochemical model and the costing methodology for the low-temperature CO_2 electrolysers and their separation units.

2.1.3 High-temperature electrocatalytic processes. High-temperature, solid-oxide electrolysis cells (SOEC), including dry electrolysis for converting CO_2 into CO, have undergone tremendous improvements over the past 15 years in terms of their electrochemical performance and long-term durability, both at the cell and stack levels.[80,81] Rather than developing a bottom-up model based on lab-scale experimental data as is done for low-temperature electrolysers (*cf.* Section 2.1.2), the focus is on Haldor Topsoe's carbon monoxide generator, eCOs™ for the SOEC modelling owing to its higher maturity (TRL 8).[82,83] The model assumes an overall conversion of 100%, heat supplied by electric heaters, and gas purification processes (>99 vol% of CO) included in the total energy consumption (8 kW h per Nm^3 of CO produced)—this is in contrast to the low-temperature electrolyser models where H_2 is consumed to supply heat to the amine absorption process for CO_2 recycling.

Based on a scenario in which the cumulative capacity continues to grow at the same rate as in the past, a specific cost of £600 kW^{-1} is assumed for the SOEC system by 2035.[84] This represents a >70% reduction from the present cost of 1200–2000 kW^{-1}.[84–88] The future capital cost of SOEC systems are perceived to be more uncertain than that of alkaline or PEM electrolysers,[89] given the limited number of installations today[84] and the anticipated technological improvements.[90] The assumption that learning from high-temperature water electrolysis systems can be transferred to high-temperature CO_2 electrolysis is consistent with the low-temperature CO_2 electrolysers above.

Refer to Section A of the Appendix for additional details about the reference SOEC electrolysers and to Section S2 of the ESI,† for further details about the SOEC performance and costing.

2.2 Techno-economic analysis

The candidate process routes are compared in terms of the levelised cost of ethylene (LCOEt, eqn (1)), which accounts for the resource consumption, the revenues from co-products, and the annualised capital costs of the plant at scale. The cash-flow calculation assumes that the plant is erected during the first year, then operated at full capacity from the second year onward. The return on investment is neglected by setting the net present value of the project to zero.

$$\mathrm{LCOEt} = \mathrm{AF}_{\mathrm{C_2H_4}} \frac{\mathrm{OpEx} + \mathrm{CapEx\ CRF}}{m_{\mathrm{C_2H_4}}} \quad (1)$$

The capital expenditures (CapEx) are annualised using a uniform capital recovery factor (CRF). The operational expenditures (OpEx) comprise the variable utility costs and the fixed operating expenses for salaries, maintenance and overheads.

The economic allocation factors (AF_j, eqn (2)) apportion the total annualised cost of a process among all the co-products ($j \in \{CH_4, C_2H_4, C_2H_6, C_3H_8, C_3H_6, C_{4+}, O_2\}$), according to their share on the overall revenue.

$$\mathrm{AF}_j = \frac{m_j\ \mathrm{Price}_j}{\sum_k m_k\ \mathrm{Price}_k} \quad (2)$$

Green chemical products are expected to be sold at a price premium compared to their fossil-based counterparts. Herein, the prices of the co-products ($Price_j$) are assumed to increase alongside the price of ethylene ($Price_{C_2H_4}$), so their relative market prices ($Ratio_j$, eqn (3)) with respect to ethylene will remain constant throughout the plant's lifetime. The expression for $AF_{C_2H_4}$ using these relative market prices is given in eqn (4).

$$\mathrm{Ratio}_j = \frac{\mathrm{Price}_j}{\mathrm{Price}_{\mathrm{C_2H_4}}} \quad (3)$$

$$\mathrm{AF}_{\mathrm{C_2H_4}} = \frac{m_{\mathrm{C_2H_4}}}{m_{\mathrm{C_2H_4}} + \sum_{j \neq \mathrm{C_2H_4}} m_j\ \mathrm{Ratio}_j} \quad (4)$$

Refer to Sections S4 and S5 of the ESI,† for further details on economic calculations.

Table 2 Nominal values of economic input parameters in the techno-economic analysis. The ranges provided for selected uncertain parameters in the sensitivity analysis assume triangular distributions. The value of $Cost_{stack}$ is only applicable to AEM cells. The rows in bold indicate that the values of $Cost_{el}$, $Cost_{H_2}$ and $Cost_{CO_2}$ are varied simultaneously in the sensitivity analysis. The higher heating value (HHV) of hydrogen (141.8 MJ kg^{-1})[106] is used

Parameter	Unit	Nominal	Range
LT	year	20	
r	—	0.06	
UF	—	0.9	
$CEPCI_{2019}$	—	607.3	
$m_{C_2H_4}$	kt $year^{-1}$	800	
$Cost_{tax}$	£ $t_{CO_2}^{-1}$	301.4	
$Cost_{tww}$	£ t_{ww}^{-1}	0.52	
$Cost_{el}$	**£ MW h^{-1}**	**54.6**	**49.9–76.7**
$Cost_{H_2}$	**£ MW h^{-1}**	**74.3**	**67.9–104.3**
$Cost_{CO_2}$	**£ $t_{CO_2}^{-1}$**	**312.3**	**301.5–363.1**
$Cost_{stack}$	£ kW^{-1}	283.5	235–782
$Ratio_{CH_4}$	—	0.13	
$Ratio_{C_2H_6}$	—	0.15	
$Ratio_{C_3H_6}$	—	0.87	0.70–1.05
$Ratio_{C_3H_8}$	—	0.39	
$Ratio_{C_{4+}}$	—	0.8	
$Ratio_{O_2}$	—	0.13	0.00–0.13

2.3 Case study and sensitivity analysis

The ethane cracker in Wilton (North Yorkshire, UK), with an annual production capacity of 800 kt, is chosen as the reference herein.[5,91] A plant lifetime of 20 years is assumed, with a utilisation factor (UF) of 90% and discount rate of 6%.[92,93] To study a transition to green ethylene in the near future, cost assumptions for 2035 are used where available, with all costs expressed in $£_{2019}$ for consistency. The economic input parameters are summarised in Table 2 and discussed below.

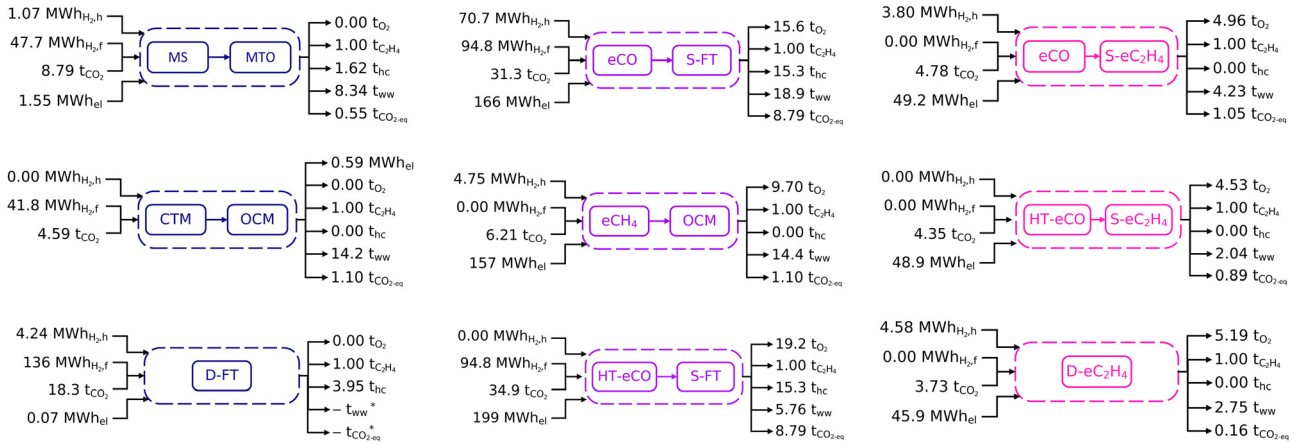

Fig. 2 Process inventories for the production of 1 t of ethylene using fully thermocatalytic routes (blue), fully electrocatalytic routes (pink) and hybrid routes (purple). The hydrogen inputs distinguish heat (H_2,h) and feedstock (H_2,f). The hydrocarbon by-products (hc) include methane, ethane, propylene, propane and C_{4+}. The waste streams consist of wastewater (ww) by the separation processes and residual GHG emissions (CO_2-eq). *Not quantified.

While such large-scale production capacity is instrumental to contextualise the electricity consumption of green ethylene (*cf.* Section 3.4 below), some of the emerging technologies may not reach kilotonne annual production levels in the near future. It is worth reiterating that the process inventories and LCOEt for each route are calculated for smaller (relevant) process scales, as dictated by their reference processes (*cf.* Section A of the Appendix). The assessment methodology therefore relies both on technology scale-up and technology scale-out.

The cost of non-intermittent electricity ($Cost_{el}$), renewable hydrogen ($Cost_{H_2}$) and air-captured CO_2 ($Cost_{CO_2}$) are based on a common value for the levelised cost of electricity (LCOE) of offshore wind in the UK.[75] Balancing intermittency using both short- and long-term storage for the uninterrupted supply of renewable electricity is assumed to add 30% on top of the LCOE.[94] The price of domestically produced green H_2 is based on the LCOE using PEM electrolysers with an efficiency of 1.3 MW h_{el} MW $h_{H_2,HHV}^{-1}$, and adding an extra 36% for capital and operating costs of the electrolysers.[75] Given the proximity of underground salt caverns to the Wilton production site[95] and existing plans to build a hydrogen pipeline network in the North East of England by 2030,[96] additional charges for transport and storage are henceforth neglected.[97,98] For the ethylene product to be considered green, only CO_2 from DAC is deemed a suitable feedstock. A cost of £312.3 $t_{CO_2}^{-1}$ is estimated on the assumption that solid sorbent-based DAC is deployed at scale by 2035, including automated manufacturing of the CO_2 collectors and based on the average relative humidity and temperatures in the UK,[99] which is six-times higher than the cost for CO_2 capture from cement.[100,101] Air and water are assumed to be free of charge. The cost of residual process emissions ($Cost_{tax}$) is based on the 2035 UK carbon price of £301.4 $t_{CO_2}^{-1}$,[102] while a generic cost of £0.52 per ton of treated wastewater ($Cost_{ww}$) is assumed.[103]

A further assumption in the economic comparison is that all the hydrocarbon co-products can be sold separately, although they are often integrated with downstream processing or combusted in existing plants.[2] The market prices of hydrocarbon co-products ($Price_j$) are based on average European market prices in 2019,[104] with the market price of ethylene itself ($Price_{C_2H_4}$) at £1000 $t_{C_2H_4}^{-1}$. The price of O_2 co-product ($Price_{O_2}$) is taken at £130 $t_{O_2}^{-1}$.[105] All of the relative prices ($Ratio_j$, eqn (3)) are assumed to remain constant throughout the plant's lifetime. Notice, in particular, that ethylene has the highest market price amongst the co-products.

To determine the extent to which the process ranking is subject to key modelling assumptions, a sensitivity analysis is conducted in terms of the LCOE, the stack cost ($Cost_{stack}$), and the relative market prices of propylene ($Ratio_{C_3H_6}$) and oxygen ($Ratio_{O_2}$) with respect to the ethylene price. A Monte Carlo simulation is conducted based on low-discrepancy Sobol sampling with 1024 scenarios, leading to a confidence interval smaller than 1.5% around the mean LCOEt value. All four uncertain factors are modelled with triangular probability distributions (*cf.* Table 2). The costs of uninterrupted renewable electricity ($Cost_{el}$), green H_2 ($Cost_{H_2}$), and CO_2 feedstock ($Cost_{CO_2}$) are assumed to be correlated with the LCOE of offshore wind, whose value ranges between current costs (£59.0 MW h^{-1}) and projections for 2050 (£38.4 MW h^{-1}).[75,107] $Cost_{H_2}$ is taken directly proportional to $Cost_{el}$ since electricity is the main driver of green H_2 price, while the variation range for $Cost_{CO_2}$ accounts for the fact that electricity contributes around 40% of the cost of the solid sorbent-based DAC process.[99] Since public data on propylene prices are limited, a range of ±20% is assumed.[58] The upper and lower bounds for O_2 price are so chosen to describe a scenario whereby the market price would decrease as a result of market saturation.[49] The stack cost is varied between the capital cost of PEM electrolyser systems in 2020[75] and projected capital cost of a large-scale plant by 2030.[31]

3 Results and discussion

3.1 Process inventories

Process inventories for the nine selected routes at scale are shown in Fig. 2, with more details about the mass and energy

balances available in Section S6 of the ESI.† All these inventories are scaled for 1 tonne of ethylene produced. Differentiated by colour, the processes correspond to three fully thermocatalytic routes (MS+MTO, CTM+OCM, D-FT), three fully electrocatalytic routes (eCO+S-eC_2H_4, HT-eCO+S-eC_2H_4, D-eC_2H_4), and three hybrid routes (eCO+S-FT, HT-eCO+S-FT, eCH_4+OCM). The input-output inventory streams comprise electricity (subscript el), carbon dioxide (subscript CO_2), hydrogen (subscripts H_2,f and H_2,h), ethylene (subscript C_2H_4), other hydrocarbons (subscript hc), oxygen (subscript O_2), wastewater (subscript ww), and residual emissions (subscript CO_2-eq).

Since CO_2 provides the carbon feedstock, the CO_2 inventories closely correlate with the total hydrocarbon production (sum of C_2H_4 and hc). Most of the unconverted CO_2 and intermediates are recycled within the process boundaries, therefore the net CO_2 feedstock requirement is largely independent of the overall conversion rates. Despite the reference processes for D-FT and S-FT being tailored towards light olefins, their ethylene yields remain low and large amounts of CO_2 are consumed in side reactions to co-products such as propylene and C_{4+}. As a result, D-FT, eCO+S-FT and HT-eCO+S-FT have higher CO_2 feedstock requirements than other routes. Likewise, the MS+MTO route has a large CO_2 requirement due to significant propylene and C_{4+} side-production. Conversely, the electrocatalytic processes eCO+S-eC_2H_4, HT-eCO+S-eC_2H_4 and D-eC_2H_4 require less CO_2 feedstock since ethylene is the single product. Even though ethylene is also the sole product of OCM, the CO_2 requirement of the CTM+OCM and eCH_4+OCM routes is intermediate as part of the unconverted methane is combusted in a turbine for electricity production, thus venting CO_2 with the exhaust gas.

Hydrogen is either consumed as reaction feedstock (H_2,f) or used as heating utility (H_2,h). Neither of the electrocatalytic processes (eCO+S-eC_2H_4, HT-eCO+S-eC_2H_4, D-eC_2H_4) nor the methane-mediated route (eCH_4+OCM) require hydrogen as feedstock since hydrogen is generated *in situ* from the humidified CO_2 feed. However, as all low-temperature electrocatalytic processes have low single-pass conversion rates, they require hydrogen to provide heat for the regeneration of the amine sorbent used in the separation of unreacted CO_2 before recycling. By contrast, the thermocatalytic processes consume hydrogen mainly as a feedstock. Given that the reactions are typically exothermic, the hydrogen feedstock is also indirectly used to meet part of the heat and electricity demands through process heat integration. However, additional hydrogen as heat utility is required for the D-FT process to preheat its large recycle stream and for the MS+MTO process despite using excess heat to preheat the reactor feed (*cf.* Section S6 of the ESI†). All of the thermocatalytic processes furthermore include turbines for converting excess reaction heat into electricity. But only for the integrated CTM+OCM process is the excess heat high enough for an electricity surplus to be generated and sold to the grid. The consumption pattern of the hybrid process eCO+S-FT reflects the characteristics of thermo- and electrocatalytic routes because significant amounts of hydrogen are consumed both as feedstock to achieve the necessary syngas composition and as heating fuel in the carbon capture process due to the low single-pass conversion of the eCO stage.

The electricity demands of the electrocatalytic and hybrid processes correlate with their cell voltages and faradaic efficiencies. Despite the high faradaic efficiency of the eCO and HT-eCO stages and the excess electricity generated in the S-FT stage (15.9 MW h_{el} per t_{CO}), eCO+S-FT and HT-eCO+S-FT have the highest electricity demand due to their large intermediate syngas stream (33.6 t_{CO} per $t_{C_2H_4}$); eCH_4+OCM comes in third position as the eCH_4 stage has by far the highest cell voltage. In contrast, the fully electrocatalytic routes eCO+S-eC_2H_4, HT-eCO+S-eC_2H_4 and D-eC_2H_4 consume 3 to 4 times less electricity than the hybrid routes. And although eCO+S-eC_2H_4, HT-eCO+S-eC_2H_4 require $10e^-$ per $mol_{C_2H_4}$ compared to $12e^-$ per $mol_{C_2H_4}$ in D-eC_2H_4, all three have similar electricity demands. For those processes having electrocatalytic conversion stages, the quantity of the oxygen by-product is commensurate to the electricity demand given the OER is the complementary half-cell reaction of the CO_2/CO reduction reaction.

A significant amount of water is formed as by-product in both thermocatalytic and electrocatalytic processes. These wastewater streams either contain traces of hydrocarbons and alcohols in the case of thermocatalytic processes or correspond to an alkaline solution in the case of electrocatalytic processes, and they require treatment before crossing the process boundaries. Although the costs for an external wastewater treatment service were included in the TEA, on-site wastewater regeneration and recycling could also be implemented to lower the water footprint of the processes. The amount of wastewater produced by thermocatalytic processes generally correlates with the amount of hydrocarbons formed. The CTM+OCM process uses large amounts of steam to dilute the OCM reactor feed and therefore generates more wastewater than the MS+MTO process. Recall also that the wastewater stream of the D-FT process could not be quantified due to incomplete mass balances (*cf.* Section A.4). But as dewatering at the S-FT reactor outlet alone produces 18.81 t_{H_2O} per $t_{C_2H_4}$, wastewater production is expected to be comparable for D-FT.

Direct (gross) emissions from the thermocatalytic processes are caused by purge streams, which are translated into CO_2-equivalents on Fig. 2; while in electrocatalytic processes, the direct emissions correspond to any residual CO_2 not captured by the mixed-amine absorption column. These direct emissions are lower than those of conventional ethane crackers (c. 0.74 t_{CO_2} $t_{C_2H_4}{}^{-1}$)[108] for both the direct electrochemical route D-eC_2H_4 and the thermochemical route MS+MTO, and slightly higher for the two-stage electrochemical routes eCO+S-eC_2H_4 and HT-eCO+S-eC_2H_4. By contrast, the hybrid processes eCO+S-FT and HT-eCO+S-FT present much larger direct emissions due to the Fischer–Tropsch synthesis having a small ethylene yield and forming a range of saleable co-products. Nevertheless, an economic allocation among these co-products (*cf.* Fig. 4 below) suggests that the direct emissions associated with ethylene would remain comparable to that of ethane cracking. Recall also that the purge stream and hence the emissions of the D-FT process could not be quantified due to incomplete mass

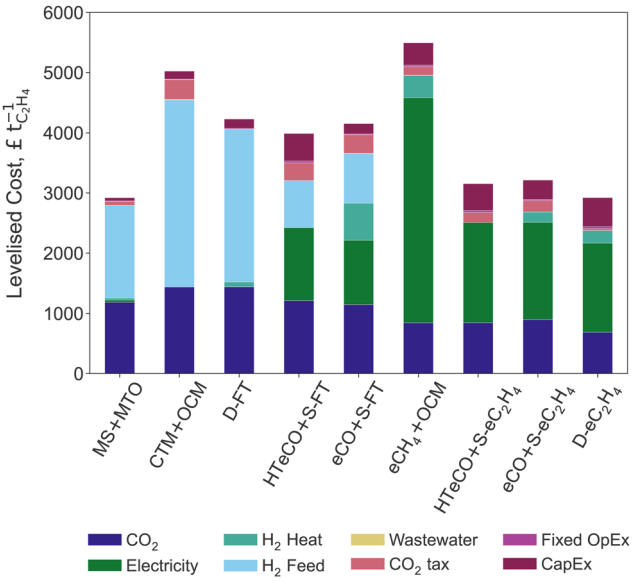

Fig. 3 Levelised cost of ethylene and corresponding breakdown for the nine candidate routes.

balances (*cf.* Section A.4). Lastly, the carbon intensity of both the CTM+OCM and eCH_4+OCM processes exceeds that of ethane cracking because significant CO_2 emissions are caused by the combustion of unconverted methane from the OCM stage to generate electricity. Although not implemented here, capturing and recycling CO_2 from this flue gas might be economically competitive given the high cost of DAC. It is also worth reiterating that the CO_2 feedstock is much larger than the direct (gross) emissions in all of the green ethylene routes and so, unlike ethane crackers, the production processes are still net CO_2 consumers. To draw final conclusions on the environmental impact, a thorough life-cycle assessment should be performed in future research.

3.2 Techno-economic comparison

The levelised costs of ethylene (LCOEt) from DAC and renewable electricity for the nine production pathways are compared in Fig. 3. The breakdown differentiates capital, fixed and variable operating costs, the latter being further differentiated into the contributions of CO_2 feedstock, renewable energy (electricity, hydrogen), wastewater treatment, and carbon tax.

The predicted LCOEt ranges between £2920–5280 $t_{C_2H_4}^{-1}$. Remarkably, both the thermocatalytic process MS+MTO and the direct electroreduction process D-eC_2H_4 provide the lowest-cost options at around £2920 $t_{C_2H_4}^{-1}$. The most expensive routes are the methane-mediated hybrids with OCM, eCH_4+OCM and CTM+OCM, both above £5000 $t_{C_2H_4}^{-1}$. The Fischer–Tropsch routes D-FT, eCO+S-FT and HT-eCO+S-FT have a comparable LCOEt in the range of £3930–4230 $t_{C_2H_4}^{-1}$. Given that the LCOEt of D-FT omits the carbon tax for direct emissions and wastewater treatment cost, its LCOEt is however underestimated. The three elecytrocatalytic routes D-eC_2H_4, eCO+S-eC_2H_4 and HT-eCO+S-eC_2H_4 also perform similarly with an LCOEt between £2920–3220 $t_{C_2H_4}^{-1}$.

Table 3 Capital expenditures (CapEx) for the nine candidate routes at a production capacity of 800 kt $year^{-1}$

Route	CapEx, $£_{2019}$Bn
MS+MTO	1.17
CTM+OCM	1.21
D-FT	5.72
HT-eCO+S-FT	37.81
eCO+S-FT	13.56
eCH_4+OCM	7.80
HT-eCO+S-eC_2H_4	6.54
eCO+S-eC_2H_4	4.88
D-eC_2H_4	7.54

All of these levelised costs can be interpreted as lower bounds on green ethylene market prices since they omit any profit margins. Even compared to a high market price of £1400 $t_{C_2H_4}^{-1}$ (recorded in April 2022)[109] and after taxing the CO_2 emissions of a conventional ethane cracker (c. £300 $t_{C_2H_4}^{-1}$ at 0.97 t_{CO_2} $t_{C_2H_4}^{-1}$), the predicted green ethylene prices are far from being competitive with fossil-based ethylene.

The routes involving an electrocatalytic conversion step generally have a higher CapEx than the thermocatalytic processes (see Table 3). The eCO+S-eC_2H_4 process achieves the lowest CapEx among the electrocatalytic and hybrid routes because it requires a relatively small electrode area given its high current density (*cf.* Section 2.1.2). It is nevertheless 4 times more expensive than MS+MTO or CTM+OCM. Despite being fully thermocatalytic, D-FT requires larger unit and equipment sizes to make up for its low ethylene yield, which is why its CapEx is comparable to that of eCO+S-eC_2H_4 and 3.5 times greater to that of S-FT. The CapEx of the electrocatalytic and hybrid processes are dominated by the CO_2/CO electrolyser cost, while the separation equipment and thermocatalytic stage contribute less than 6% and 12%, respectively.

Despite the large differences observed in Table 3, the annualised CapEx only represents a minor share of the LCOEt for any of the processes (see breakdown in Fig. 3). The contributions of the fixed OpEx are also minor as they correspond to a small percentage of the CapEx (*cf.* Section 2.2). This conclusion holds insofar as the manufacturing of CO_2/CO electrolysers can benefit from the learning rates that are predicted for PEM and SOEC electrolysers. It is also worth recalling that the assumed 5-year lifetime of the electrolyser stack by 2035 (*cf.* Section S2 of the ESI†) far exceeds current stability reports for low-temperature CO_2/CO electrolyser cells.[71,72,110,111] For instance, reducing the life-time of the D-eC_2H_4 electrolyser stack to 4 years is predicted to increase its CapEx by 19%. Therefore, extending the lifetime of the electrolyser stack is key towards improving the cost-competitiveness of electrocatalytic routes.[112]

It is clear from Fig. 3 that the cost of renewable energy---both renewable electricity and green H_2—makes up the largest share of the LCOEt across all nine routes. For the fully thermocatalytic routes (MS+MTO, CTM+OCM, D-FT), green H_2 contributes over 50% of the LCOEt. Instead, renewable electricity contributes about 50% of the LCOEt for the fully electrocatalytic routes (eCO+S-eC_2H_4, HT-eCO+S-eC_2H_4, D-eC_2H_4). The LCOEt of the hybrid route eCH_4+OCM is also dominated by the

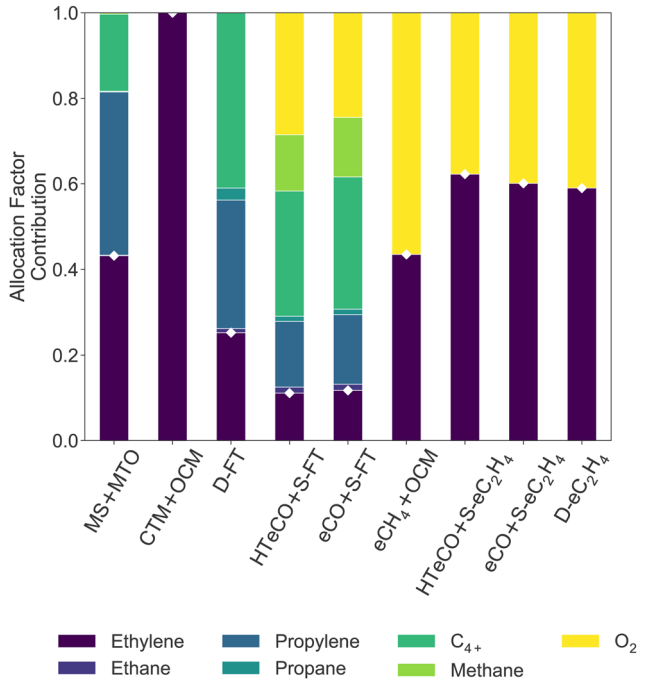

Fig. 4 Economic allocation factors AF_j (eqn (2)) of the saleable co-products in all nine candidate routes. The allocation factor of ethylene ($AF_{C_2H_4}$, white diamonds) determines the LCOEt (eqn (1)).

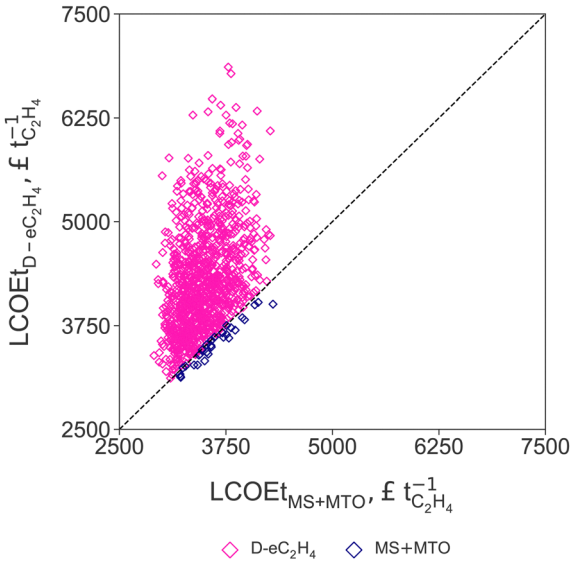

Fig. 5 Parity plot comparing the levelised cost of ethylene (LCOEt) for the thermocatalytic production of ethylene *via* methanol (MS+MTO, on *x*-axis) and direct CO_2 electroreduction to ethylene (D-eC_2H_4, on *y*-axis) for each uncertainty scenario. The levelised cost of electricity (LCOE), AEM stack cost, and market prices of propylene and oxygen are varied simultaneously (*cf.* Table 2).

electrochemical stage eCH_4 due to its high cell voltage (*cf.* Table 1), while the procurement of hydrogen and electricity both contribute significantly to the LCOEt of eCO+S-FT and HT-eCO+S-FT. Except for eCO+S-FT (15%), the contribution of hydrogen as a heating utility to the LCOEt remains below 7%.

In all nine candidate routes, the CO_2 feedstock has a notable contribution on the LCOEt because of the high cost of DAC. Substituting CO_2 from DAC for fossil-based CO_2 could reduce the share of CO_2 feedstock to 3–10% of the LCOEt, thereby making its contribution significantly smaller than the cost of green electricity or hydrogen. Conversely, the residual emissions make a minor contribution to the LCOEt in any of the selected routes, not only for a carbon tax of £301.4 $t_{CO_2}^{-1}$ (Table 2) but also in the high price scenario of BEIS with £504 $t_{CO_2}^{-1}$ by 2035.[102] Making MS+MTO cost-competitive with ethylene from a conventional ethane cracker (c. 0.74 t_{CO_2} $t_{C_2H_4}^{-1}$) would entail a carbon price of £640 t_{CO2}^{-1} or higher.

While the processes differ in conversion and ethylene yield, the LCOEt is ultimately governed by its economic allocation factor ($AF_{C_2H_4}$, eqn (4)), which reflects the relative market prices of the co-products. A breakdown of the economic allocation factor for all nine routes is shown on Fig. 4. CTM+OCM is the only selected route with ethylene as the single saleable product ($AF_{C_2H_4}$ = 100%). All the electrocatalytic routes produce oxygen as a saleable by-product alongside the desired carbon monoxide or hydrocarbons, leading to $AF_{C_2H_4}$ values between 45–65%. Propylene and C_{4+} are the dominant co-products of the thermochemical routes MS+MTO and D-FT as well as the hybrid route eCO+S-FT. While MS+MTO has an $AF_{C_2H_4}$ value over 40%, those of the Fischer–Tropsch syntheses are much lower due to low ethylene yields.

Based on this techno-economic comparison, it is unlikely for green ethylene production involving a Fischer–Tropsch synthesis (D-FT, eCO+S-FT, HT-eCO+S-FT) to be cost-competitive with other thermocatalytic processes, unless the value of its co-products or its conversion rate were to increase significantly. Neither of the OCM routes (CTM+OCM, eCH_4+OCM) is furthermore competitive with MS+MTO given that OCM does not produce any other valuable hydrocarbon products than ethylene. The cost advantage of MS+MTO over CTM+OCM, eCH_4+OCM or D-FT is consistent with previous techno-economic assessments.[44,45]

Finally, the LCOEt of all three electrocatalytic routes (eCO+S-eC_2H_4, HT-eCO+S-eC_2H_4, D-eC_2H_4) is within 10% of that of MS+MTO. This gap would increase significantly if the oxygen by-product from the electrolysers could no longer be valorised or if the life-time of the electrolyser stack did not extend beyond 3 or 4 years, as already noted. A single-pass conversion lower than the assumed 40% in AEM electrolysers (*cf.* Table 1) would also be detrimental to the LCOEt, due to the combined effect of increasing H_2 consumption to recycle unconverted CO_2, CO_2 feed and CO_2 emissions. For instance, a 30% single-pass conversion would already increase the LCOEt of both D-eC_2H_4 and eCO+S-eC_2H_4 by 5%. The overall similarity in LCOEt between eCO+S-eC_2H_4, HT-eCO+S-eC_2H_4 and D-eC_2H_4 is in agreement with recent techno-economic assessments, albeit conducted under different system boundaries.[48,113] If it were not for the high electrolyte molarity (7 M KOH) in the selected D-eC_2H_4 reference (*cf.* Section A.4 of the Appendix),[72] D-eC_2H_4 might as well rank behind the two tandem routes eCO+S-eC_2H_4 and HT-eCO+S-eC_2H_4. For instance, in a scenario with 1 M KOH electrolyte and target cell voltage of 3.5 V,[114,115]

the LCOEt of D-eC_2H_4 would already increase by 17% (£3600 $t_{C_2H_4}^{-1}$).

3.3 Sensitivity analysis

Results from the Monte Carlo analysis results for the two routes with the lowest LCOEt (MS+MTO and D-eC_2H_4) are summarised in Fig. 5, where uncertainties in the LCOE, stack cost, and market prices of propylene and oxygen relative to the ethylene price are varied simultaneously (*cf.* Section 2.3). The parity plot confirms that the production cost of the MS+MTO process remains the lowest across the range of sampled uncertainty scenarios. Only in scenarios with low propylene price, low stack cost, high LCOE and high oxygen price, does the LCOEt of D-eC_2H_4 become comparable to that of MS+MTO. This scenario analysis also reveals that the production cost of green ethylene at three times the current market price of (fossil-based) ethylene corresponds to a rather favourable scenario, due in large part to the skewed distributions of LCOE, stack cost and oxygen price.

Recall that varying the LCOE of offshore wind between current costs (£59.0 MW h^{-1}, +40%) and projections for 2050 (£38.4 MW h^{-1}, −9%) changes the cost of non-intermittent renewable electricity, green hydrogen and air-captured CO_2 proportionally (*cf.* Section 2.3). The LCOEt of both MS+MTO and D-eC_2H_4 processes correlate linearly with the LCOE (Fig. 6A). In particular, the ranking between MS+MTO and D-eC_2H_4 is preserved over the whole LCOE range. D-eC_2H_4 could become the cheapest option if the faradaic efficiency were to reach 80% (from the nominal 66% efficiency). But if PEMs were used instead of AEMs, the cell potential would increase by 25%, and the LCOEt gap between the two processes would widen; as it would if the electrolyte molarity was reduced to 1 M KOH (from the nominal 7 M KOH, *cf.* Section 3.2). Nevertheless, a more detailed modelling would be required to quantify the potential benefits afforded by adapting the operation of D-eC_2H_4 to fluctuating electricity prices.

Reducing the stack cost from current prices to costs projected for 2030 would help close the LCOEt gap, but still not enough for D-eC_2H_4 to overtake MS+MTO (Fig. 6B). For D-eC_2H_4 to gain a competitive advantage over MS+MTO, reductions by over 12% in electricity consumption would be necessary, through improvement in faradaic efficiency and cell voltage. Given that the annualised CapEx contributes only 17% to the LCOEt (Fig. 3), the LCOEt of D-eC_2H_4 is however more sensitive to variations in the relative market price of oxygen than it is to the stack cost (compare Fig. 6B and D).

The large amount of oxygen by-product (5.2 t_{O_2} $t_{C_2H_4}^{-1}$) makes its market price decisive for the economic allocation factor of D-eC_2H_4 (*cf.* Section 3.2). If the oxygen price were to drop as a consequence of market saturation, the LOCEt of D-eC_2H_4 would increase, even causing the LCOEt to double in scenarios where the oxygen price is null (Fig. 6C). Similarly, if the market price of oxygen were to remain at today's level (£130 $t_{O_2}^{-1}$) while the market price of green ethylene tripled (£3000 $t_{C_2H_4}^{-1}$), the LCOEt of D-eC_2H_4 would be double that of MS+MTO.

Propylene is the main saleable co-product of the MS+MTO route and thereby influences the economic allocation factor. A negative correlation between the price ratio and the LCOEt is observed in Fig. 6D. But with about 1 $t_{C_3H_6}$ produced for each $t_{C_2H_4}$, propylene price variation exerts a smaller effect on MS+MTO than the oxygen price does on D-eC_2H_4 (compare Fig. 6C Even for a propylene price on par with ethylene, as observed for instance in April 2022,[116] the LCOEt from MS+MTO would only decrease by a mere 2.3%.

Our finding that MS+MTO remains the lowest-cost process for green ethylene production across the majority of simulated scenarios suggests that scaling up of the current best available CO_2 electrolysers may not be enough for producing low-cost green ethylene and significant performance improvement is needed for electrocatalytic routes to become competitive with MS+MTO. National green hydrogen production targets carry an additional risk to the competitiveness of D-eC_2H_4 as oxygen is also a by-product of water electrolysis. If the UK's ambitious target of 10 GW of low-carbon hydrogen production were to be produced in the form of green hydrogen, an extra 2 Mt_{O_2} per year would be added to the market by 2030. Without a concurrent increase in demand, *e.g.* for oxy-combustion[117] or in wastewater treatment applications,[118] the oxygen market price could drop. Meanwhile, the prices of green ethylene produced by MS+MTO could drop if the propylene price were to rise. Since ethylene and propylene are predominantly co-produced in naphtha crackers, their prices in the European market are currently highly correlated. But this interdependence could weaken in the future if the defossilisation of ethylene and propylene relied on separate feedstock. As indicated by the cost breakdown in Fig. 3 though, the LCOE from renewable power generators remains the most sensitive factor for competitive green ethylene prices by and large.

3.4 Beyond the process boundaries

At the time this paper is written, all three ethane steam crackers in the UK are reliant on shale gas imports from the US.[119,120] CO_2 utilisation for ethylene production therefore would promote the use of local resources such as offshore wind power. But a major impediment to the deployment of green ethylene lies with the huge demand for renewable electricity. The modelling conducted in the previous sections predicts that MS+MTO and D-eC_2H_4 would consume, respectively, 52 TW h_{el} and 41 TW h_{el}—assuming an efficiency of 1.3 MW h_{el} MW $h_{H_2,HHV}^{-1}$ for PEM electrolysers—to displace a single cracker with an annual capacity of 800 kt. In particular, these demands correspond to 13–16% of the UK's total electricity generation in 2022 (325 TW h_{el}).[121] On top of this, powering the DAC plant for MS+MTO and D-eC_2H_4 would require an additional 14 TW h_{el} and 6 TW h_{el} of renewable electricity, respectively, even with efficient heat pump systems and assuming an average electricity requirement of 2 MW h_{el} $t_{CO_2}^{-1}$.[99] These figures also need to be contrasted with our reference ethane cracker in Wilton (UK) consuming 11.5 TW h_{el} per year in total,[6] a much smaller share (c. 3.5%) of the UK's annual electricity consumption.

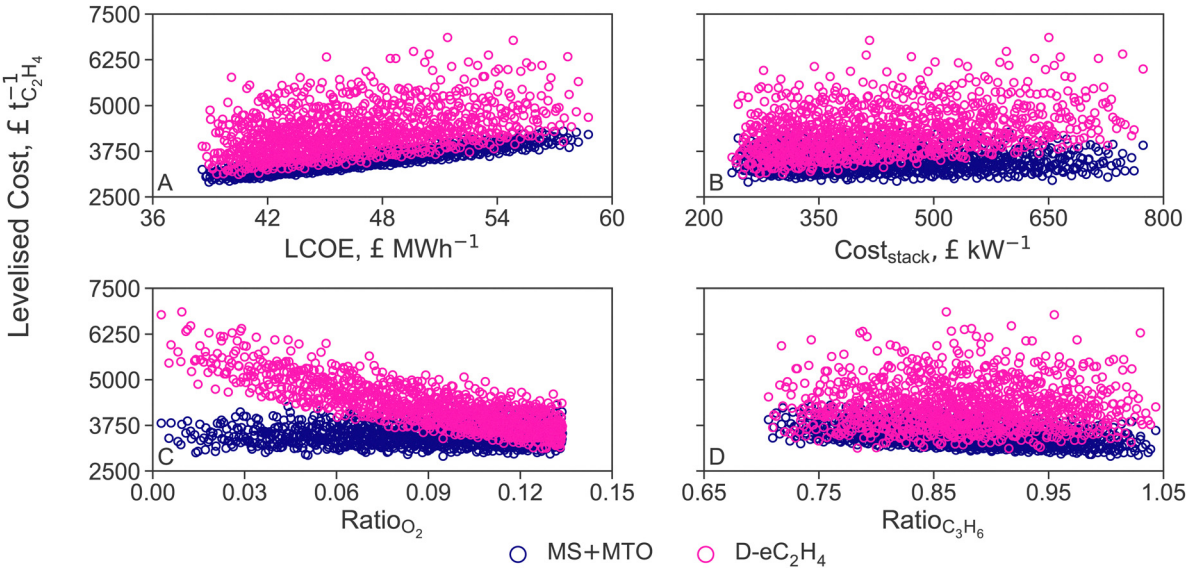

Fig. 6 Sensitivity analysis of the levelised cost of ethylene (LCOEt) to variations in the levelised cost of electricity (LCOE, A), AEM stack cost (B) and market prices of oxygen (C) and propylene (D) for the thermocatalytic production of ethylene *via* methanol (MS+MTO) and direct CO_2 electroreduction to ethylene (D-eC$_2$H$_4$). The costs of hydrogen and CO_2 feedstock are varied simultaneously with LCOE (*cf.* Table 2).

Alongside the huge demand for renewable energy to power green ethylene comes the physical footprint of a dedicated offshore wind farm. Assuming an average power per unit area of 3 W m^{-2} in the UK,[122] the required offshore area would be 2800 km^2 for MS+MTO and 2000 km^2 for D-eC$_2$H$_4$, corresponding to 1.2–1.7 times the area of Greater London.[123] Such figures put a clear pressure on the chemical industry to take a strategic decision on securing its supply of low-cost, low-carbon electricity. Delaying this decision could put the industry at risk of missing out on the best offshore wind farm leases, as the seabed areas in the UK exclusive economic zone (EEZ) are continuously auctioned. In the context of low-carbon ethylene production, the chemical industry might want to reconsider the idea of co-locating future chemical plants with nuclear plants that could supply both heat and power.[124]

Both geographic and geological characteristics govern the cost of green ethylene production. Like the UK, Northern Germany and Denmark have large offshore wind potentials in close proximity to underground salt caverns for low-cost, large-capacity hydrogen storage.[125] Therefore, a LCOEt similar to our case study (Fig. 3) could be expected for production sites in those countries. While salt caverns are also available offshore in the North Sea, higher cost for offshore solution mining, injection wells and pipelines would exacerbate the cost of hydrogen storage. For production sites where geological hydrogen storage is unavailable, the use of pressure tanks could increase the hydrogen cost by 20%,[98] in turn increasing the LCOEt of MS+MTO by 10%.

At the global level, the production cost of green ethylene will be dependent on the availability of renewables, climatic conditions, and financing conditions all together. Outside Europe, the Western US might offer suitable conditions for a similar LCOEt as in the UK (Fig. 3), but given that fossil-based ethylene in the US is less than half the price on the European market,[126] green ethylene would be even less competitive on the US market. Comparable LCOE and LCOH to the UK could also be achieved in other parts of the World, such as the West Coast of Canada, the Arabic Peninsula or Australia.[127,128] Nevertheless, the climatic conditions there would make CO_2 capture using solid sorbent-based DAC 10–25% more expensive.[99] A more detailed and systematic assessment is necessary to identify favourable locations for green ethylene production.

When deciding between D-eC$_2$H$_4$ and MS+MTO for the production of green ethylene, not only the cost but also the supply security during dark doldrums, periods in which little to no electricity is generated by offshore wind farms, should be considered. Renewable electricity is a localised resource that may not be transported over long-distances and for which supply and demand need to be matched at any point in time. Instead, local production of green hydrogen could be supplemented by imports from countries with similar or lower predicted production costs, such as Algeria and Australia.[128,129] Even though hydrogen imports could also be reconverted to electricity for D-eC$_2$H$_4$, the associated losses would make it more cost-effective to directly use hydrogen in the MS+MTO process. For a future in which the chemical industry is mainly reliant on renewable power, a higher diversity of supply could bring greater price stability, as the price of commodity chemicals such as ethylene are otherwise at risk of becoming weather-dependent.

Finally, the main motivation behind displacing fossil-based ethylene for green ethylene lies in the prospect of producing carbon-negative ethylene and co-products (use phase excluded). To calculate the net CO_2 emissions, the CO_2 inlet streams are subtracted from the sum of scope-1 residual emissions and scope-2 emissions associated with electricity that is consumed either directly or for the production of H_2 and CO_2. Assuming an average carbon intensity of 7.5 $kg_{CO_2\text{-eq}}$ MW h_{el}^{-1},[130] the

allocated net emissions per tonne of ethylene produced amount to −3.3 $t_{CO_2\text{-eq}}$ for MS+MTO and −1.9 $t_{CO_2\text{-eq}}$ for D-eC_2H_4. Both thermocatalytic and electrocatalytic routes would thus present a negative carbon balance from a cradle-to-gate point of view. On the path to net-zero, this would allow for a dramatic reduction over conventional ethane steam crackers, whose cradle-to-gate emissions are estimated to exceed 3 $t_{CO_2\text{-eq}}$ per tonne of ethylene with ethane from shale gas.[108] A cradle-to-grave assessment encompassing the ethylene use phase in consumer products and any downstream emissions is nevertheless required to conclude on the negative emission potential of green ethylene as a whole.[131]

4 Conclusions

A techno-economic comparison between mature thermocatalytic and novel electrocatalytic processes was conducted for the production of green ethylene from air-captured CO_2 and offshore wind electricity, with a view to displacing a conventional ethane cracker in the UK at the horizon of 2035. Similar to fossil-based processes today, the production cost of green ethylene would be dominated by the cost of energy and carbon feedstock, regardless of the process alternative. The fully-thermocatalytic route converting CO_2 to methanol then to olefins would achieve the lowest cost (£2900 $t_{C_2H_4}^{-1}$), followed by fully-electrocatalytic routes (£2900–3200 $t_{C_2H_4}^{-1}$). Process routes relying on Fischer–Tropsch synthesis or oxidative coupling of methane would furthermore be non-competitive. Although considering a UK case study herein, similar levelised cost of green ethylene are expected in Northern Germany or Denmark.

Apart from the levelised cost of electricity, the market price of the oxygen by-product and electrolyser stack cost are identified as key sensitive factors to the cost-competitiveness of the electrocatalytic processes. However, the methanol-mediated thermocatalytic route is predicted to out-compete the direct electroreduction of CO_2 to ethylene, even for scenarios of high oxygen prices and low stack cost. From a cradle-to-gate perspective, both processes have the potential to reduce the carbon emissions of ethylene production significantly and achieve net-negative emissions between −3.3 to −1.9 $t_{CO_2\text{-eq}}$. But a major barrier to green ethylene deployment lies in its energy-intense nature, making it highly reliant on a large-scale supply of low-cost renewable electricity. Displacing a single cracker with an annual production capacity of 800 $kt_{C_2H_4}$ would consume the equivalent of 14–20% of the UK's current power generation and require an offshore wind farm larger than the area of Greater London. Finally, transitioning from fossil fuels to intermittent renewable electricity requires a rethinking of the supply security of chemical processes, especially during dark doldrums. The process inventories developed herein could feed into decision-support models for analysing the wider consequences of ethylene defossilisation for the UK's future energy system. As an interim solution, ethylene production will continue to rely on fossil feedstock but could be retrofitted with CCS or H_2 as fuel to lower its emission intensity.

Nomenclature

Acronyms

CO_2RR	Electroreduction of CO_2
CORR	Electroreduction of CO
AEM	Alkaline electrolyte membrane
AF	Allocation factor
UF	Utilisation factor
ASU	Air separation unit
BEIS	Department for Business, Energy & Industrial Strategy
BOP	Balance of plant
CapEx	Capital expenditures
CCS	Carbon capture and storage
CEPCI	Chemical engineering plant cost index
CRF	Capital recovery factor
DAC	Direct air capture
EEZ	Exclusive economic zone
FT	Fischer–Tropsch
FE	Faradaic efficiency
GHG	Greenhouse gas
HHV	Higher heating value
LCA	Life-cycle assessment
LCOE	Levelized cost of electricity
LCOEt	Levelized cost of ethylene
LCOH	Levelized cost of hydrogen
OER	Oxygen evolution reaction
OpEx	Operational expenditures
PEM	Proton exchange membrane
PTFE	Polytetrafluoroethylene
SOEC	Solid oxide electrolysis cell
TIC	Total invested capital
TRL	Technology readiness level
UK	United Kingdom
US	United States
VPSA	Vacuum pressure swing adsorption

Subscripts

el	Electricity
eq	Equivalents
f	Feedstock
h	Heating
hc	Hydrocarbons other than ethylene
stack	Electrolyser stack
tax	Carbon tax
ww	Wastewater

Model parameters and variables

η_F	Faradaic efficiency
LT	Lifetime
E_{cell}	Cell voltage
E_{red}	Reduction potential
$f_{O\&M}$	Share of fixed operating costs on CapEx
j	Current density
m_j	Production rate of product j
r	Interest rate
X	Conversion
AF_j	Allocation factor of co-product j

A_{cell}	Area of the electrode
$Cost_j$	Unit cost of process input/emission j
$Price_j$	Market price of co-product j
$Ratio_j$	Ratio of market price of co-product j to ethylene

Process technologies

CTM	CO_2 methanation
D-eC_2H_4	Direct electroreduction of CO_2 to ethylene
D-FT	Direct Fischer–Tropsch synthesis
eCH_3OH	Electroreduction of CO_2 to methanol
eCH_4	Electroreduction of CO_2 to methane
eCO	Electroreduction of CO_2 to CO
HT-eCO	High-temperature electroreduction of CO_2 to CO
MS	Methanol synthesis
MTO	Methanol to olefins
OCM	Oxidative coupling of methane
S-eC_2H_4	Electroreduction of CO to ethylene
S-FT	Syngas Fischer–Tropsch synthesis

Author contributions

Andreas H. Nyhus: data curation, formal analysis, methodology, validation, software, investigation, visualisation, writing – original draft preparation. Maria Yliruka: conceptualisation, supervision, data curation, methodology, investigation, validation, writing – original draft preparation, writing – reviewing and editing. Nilay Shah: funding acquisition, writing – reviewing and editing. Benoît Chachuat: supervision, validation, writing-reviewing and editing.

Data availability

Data is available upon request.

Conflicts of interest

There are no conflicts to declare.

Appendix

A Green ethylene production routes

This appendix provides further details about the selected reference processes in the conversion of CO_2 to green ethylene (*cf.* Fig. 1). TRLs of these processes are summarised in Table 4.

A.1 Methanol intermediate route

Methanol synthesis (MS). Production of methanol *via* CO_2 hydrogenation (reactions (5) and (6)) has reached TRL 9, with commercial plants already operating in China.[132] CO_2 and H_2 flow over a Cu/ZnO/Al_2O_3 catalyst in a fixed bed reactor under 76 bar and 210 °C to form methanol at a purity of 99.9 wt%.[93]

$$CO_2 + 3H_2 \rightleftharpoons CH_3OH + H_2O \quad (5)$$

$$CO_2 + H_2 \rightleftharpoons CO + H_2O \quad (6)$$

The CO_2 hydrogenation to methanol process was modelled by Matzen *et al.*,[133] Wiesberg *et al.*,[134] and Pérez-Fortes *et al.*[93] The first was discarded as the levelised capital cost (£65.1 t^{-1}) was significantly larger than those in Wiesberg *et al.*[134] (£20.5 t^{-1}) and Pérez-Fortes *et al.*[93] (£19.3 t^{-1}). Since Wiesberg *et al.*[134] did not integrate the waste heat of the reactor, the process model from Pérez-Fortes *et al.*[93] minimising exergy losses was selected as reference.

Table 4 Technology readiness level (TRL) of the process candidates. Refer to Fig. 1 for a list of abbreviations

Process	TRL
MS	9
eCH_3OH	4
MTO	9
CTM	9
eCH_4	4
OCM	6
eCO	4
HT-eCO	8
S-FT	4
S-eC_2H_4	4
D-FT	4
D-eC_2H_4	4

CO_2RR to methanol (eCH_3OH). Electroreduction of CO_2 to methanol (half-cell reactions (7) and (8)) over a Cu catalyst[135] is most effective with a proton-exchange membrane (PEM) and alkaline electrolyte in a flowing cell set-up (TRL 4).[136–139]

$$CO_2 + 6H^+ + 6e^- \rightarrow CH_3OH + H_2O \quad (7)$$

$$3H_2O \rightarrow \frac{3}{2}O_2 + 6H^+ + 6e^- \quad (8)$$

In contrast to other electrocatalytically produced intermediates, methanol is found in the electrolyte together with water and formic acid as common side-products.[137] Based on the low single-pass production rate (3.2×10^5 mol m^{-2} s^{-1}) reported in Albo *et al.*,[140] the electrolyte would need too large a recirculation ratio in order to increase methanol concentration before distillation. This route was therefore excluded from further analysis on the basis of technical infeasibility.

Methanol to olefins (MTO). Production of light olefins from methanol is at TRL 9, with commercial plants in operation in China.[141] A SAPO-34 catalyst[142] enables the conversion of methanol and steam at 3 bar and 400 °C to light olefins, achieving close to 100% conversion and 80% selectivity to ethylene and propylene at a product purity of 99.5 wt%.[143] The hydrocarbon products [CH_2] are formed *via* the dimethylether intermediate CH_3OCH_3 according to a complex exothermic reaction scheme,[142] as summarised in reaction (9).

$$2CH_3OH + H_2O \rightleftharpoons CH_3OCH_3 \rightleftharpoons [CH_2] + H_2O \quad (9)$$

Economic analyses of the MTO process are found in Jasper *et al.*[144] and Chen *et al.*[143] The first was discarded as the authors significantly simplified the actual plant by adjusting stream compositions using hydrocarbon imports and simplifying the separation train to three columns instead of five.[142] Of the two designs presented in Chen *et al.*,[143] the optimised

design was chosen as reference due to its much reduced energy requirement of 0.56 GJ t^{-1} compared to 1.51 GJ t^{-1} in the second one.

A.2 Methane intermediate route

CO_2 methanation (CTM). Methanation of CO_2 has been commercially operated in Germany since 2013,[145] thus considered TRL 9. Methane is formed by reacting H_2 and CO_2 in a stoichiometric ratio of 4 (reactions (6), (10) and (11)) over a Ni/$MgAl_2O_4$ catalyst in an adiabatic fixed-bed reactor at 10 bar and at 350 °C.[92]

$$CO_2 + 4H_2 \rightleftharpoons CH_4 + 2H_2O \quad (10)$$

$$CO + 3H_2 \rightleftharpoons CH_4 + H_2O \quad (11)$$

Both Chauvy *et al.*[92] and Iaquaniello *et al.*[146] modelled CO_2 methanation to produce synthetic natural gas using power-to-gas technology. The latter considered feeding a flue gas stream containing only 8.7 vol% CO_2 and was discarded since the reactor and separation train would be significantly oversized as a result. By contrast, the CO_2 feed stream in Chauvy *et al.*[92] was 98 mol% pure, so it was selected as reference.

CO_2 electroreduction to methane (eCH_4). Electroreduction of CO_2 to methane (half-cell reactions (12) and (13)) appears as the most immature technology of all the considered CO_2RR routes (TRL 4). Recent research has been more focused on other CO_2RR products such as CO or C_2H_4 than CH_4.[147]

$$CO_2 + 6H_2O + 8e^- \rightarrow CH_4 + 8OH^- \quad (12)$$

$$8OH^- \rightarrow 2O_2 + 4H_2O + 8e^- \quad (13)$$

For the electrocatalytic conversion of CO_2 to CH_4, Zhang *et al.*[70] achieved high current densities by coating the Cu/CuO_x catalyst with a hydrophobic carbon shell, while Pan *et al.*[148] achieved low cell voltage and high faradaic efficiency using a Nafion-covered Cu-electrode. The work by Zhang *et al.*[70] was selected over Pan *et al.*[148] given the reported high faradaic efficiency and a two orders of magnitude higher current density (5000 A m^{-2}). Zhang *et al.*[70] has the highest current density out of the papers reviewed by Li *et al.*[147]

Oxidative coupling of methane (OCM). This process was demonstrated at pilot scale (TRL 6) by Siluria Technologies in the US.[149] Ethylene is produced by reacting CH_4 and O_2 (reactions (14)–(16)) over a Na_2WO_4-Mn/SiO_2(W-Mn/SiO_2) catalyst in a cooled reactor with inlet at 350 °C and outlet at 305 °C under 9 bar.[150]

$$2CH_4 + \tfrac{1}{2}O_2 \rightleftharpoons C_2H_6 + H_2O \quad (14)$$

$$C_2H_6 + \tfrac{1}{2}O_2 \rightleftharpoons C_2H_4 + H_2O \quad (15)$$

$$C_2H_6 \rightleftharpoons C_2H_4 + H_2 \quad (16)$$

Both Spallina *et al.*[150] and Layritz *et al.*[151] modelled OCM as a decarbonisation route for conventional naphtha crackers. The second was discarded because the capital cost of the OCM reactor could not be separated from the total system cost. Of the five process designs compared in Spallina *et al.*,[150] the reference was chosen as the design optimised for a lower operating temperature.

A.3 Carbon monoxide intermediate route

Low-temperature CO_2 electroreduction to CO (eCO). Common amongst experimental studies on CO_2 electroreduction to CO (half-cell reactions (17) and (18); TRL 4) is the use of a flowing alkaline electrolyte,[152–154] sometimes paired with an ionic liquid.[155,156] Candidate transition metal catalysts include Zn,[153] Ni,[154] Ag,[155] Co,[69] and Au.[157]

$$CO_2 + H_2O + 2e^- \rightarrow CO + 2OH^- \quad (17)$$

$$2OH^- \rightarrow \tfrac{1}{2}O_2 + H_2O + 2e^- \quad (18)$$

Wang *et al.*[69] achieved high faradaic efficiency and current density with a CoN_4 catalyst on carbon nanotubes in an alkaline electrolyte membrane (AEM), while Verma *et al.*[157] reported low cell voltage with an Au catalyst on polymer and carbon nanotubes also in an AEM. The former was chosen since the reported current density (3500 A m^{-2}) was 14-times higher.

High-temperature CO_2 electroreduction to CO (HT-eCO). SOEC technology relies heavily on decades-long research and development effort that has gone into commercialising solid oxide fuel cells (SOFC). It has reached TRL 8 for dry electrolysis of CO_2 to CO (half-cell reactions (19) and (20)), for instance with Haldor Topsoe's patented carbon monoxide generator, eCOs™ for small-scale applications.[83,158] This high-temperature electrolysis operates at 600–850 °C where it benefits from a reduced theoretical minimum cell voltage and faster reaction kinetics.[80] In contrast to low-temperature CO_2 electrolysers which require a liquid (aqueous) electrolyte, the oxide ions migrate through a ceramic electrolyte in a SOEC, most commonly Y_2O_3-stabilised ZrO_2 (YSZ). The CO_2 electrode needed to conduct both ions and electrons is therefore a ceramic-metal material, usually Ni-YSZ.[159] Often separated by gadolinium-doped cerium oxide layer,[160] a layer of lanthanum strontium manganite (LSM) perovskite can serve as the anode.[161]

$$CO_2 + 2e^- \rightarrow CO + O^{2-} \quad (19)$$

$$O^{2-} \rightarrow \tfrac{1}{2}O_2 + 2e^- \quad (20)$$

The selected SOEC model relies on public data reported by Haldor Topsoe,[158] specifically the upper bound on the total energy consumption (8 kW h per Nm^3 of CO produced) in order to achieve a high-purity CO stream (>99% purity).

Syngas Fischer–Tropsch synthesis (S-FT). While FT synthesis is already used at commercial scale for fuel production, its application in olefins production is still at the research stage (TRL 4).[162,163] The exothermic conversion of syngas to low olefins (reaction (21)) over a Fe–Mn–Cu–K catalyst has been reported under 10 bar and 330 °C.[57]

$$nCO + nH_2 \rightarrow [CH_2]_n + nH_2O \quad (21)$$

Liu *et al.*[57] and Xiang *et al.*[164] both studied Fischer–Tropsch synthesis of olefins, including the generation of syngas from fossil-fuels within the system boundary. The former was

selected as reference since the natural gas reforming step could be excluded from the rest of the process.

CO electroreduction to ethylene (S-eC$_2$H$_4$). Cu has emerged as the catalyst of choice for CO reduction to ethylene under alkaline conditions (half-cell reactions (22) and (23)) in lab-scale electrolysers (TRL 4).[71,165–167]

$$2CO + 4H_2O + 8e^- \rightarrow C_2H_4 + 8OH^- \quad (22)$$

$$8OH^- \rightarrow 2O_2 + 4H_2O + 8e^- \quad (23)$$

Ji *et al.*[71] reported low cell voltage with a Cu on polymer catalyst in an AEM, while Duong *et al.*[165] achieved high faradaic efficiency with a dendritic Cu catalyst in an AEM. The current densities reported in both studies were similar, so the former was chosen as reference since the reported cell voltage (2.01 V) was about half.

A.4 Direct route

Direct Fischer–Tropsch synthesis (D-FT). Similar to FT synthesis of low olefins from syngas (S-FT), the development of a bifunctional catalyst for direct FT synthesis from CO_2 (reactions (6) and (21)) remains at the research stage (TRL 4).[168–170] Direct conversion of CO_2 and H_2 to ethylene through FT was also reported using a Fe-K/γ-Al_2O_3 catalyst under 10 bar and 300 °C.[171] Do and Kim[172] recently designed a heat-integrated process using this Fe-K/γ-Al_2O_3 catalyst, which was selected as reference. Nevertheless the mass balances provided by Do and Kim[172] are incomplete in that they do not allow quantifying the purge and wastewater streams from D-FT.

CO_2 electroreduction to ethylene (D-eC$_2$H$_4$). Similar to CO electroreduction to ethylene, research on direct electroreduction of CO_2 to ethylene (half-cell reactions (24) and (25)) has converged on Cu as the catalyst of choice, with operation under flowing alkaline conditions (TRL 4).[110,173]

$$2CO_2 + 8H_2O + 12e^- \rightarrow C_2H_4 + 12OH^- \quad (24)$$

$$12OH^- \rightarrow 3O_2 + 6H_2O + 12e^- \quad (25)$$

Dinh *et al.*[72] and Li *et al.*[114] both reported ethylene production with high faradaic efficiency and current density under low cell voltage. Dinh *et al.*[72] devised a multilayer graphite/carbon nanoparticles/Cu/PTFE electrode, while Li *et al.*[114] used a Cu–ligand catalyst on an AEM. Since the current densities (1100 A m^{-2} and 1390 A m^{-2}, respectively) are close, the cell voltages (1.78 V and 2.03 V, respectively) became the decisive criterion, making Dinh *et al.*[72] the chosen reference. Though it is important to note that the current density in this reference was collected in a flow cell with a 7 M KOH electrolyte, so reducing the electrolyte molarity for scaling-up production could incur much greater ohmic losses and increase the cell voltage in turn.

Acknowledgements

Maria Yliruka is funded by the UK Engineering and Physical Sciences Research Council (EPSRC) under grant EP/R045518/1. Benoît Chachuat and Nilay Shah gratefully acknowledge funding by the EPSRC under grants EP/V011863/1 and EP/V042432/1. The authors would like to thank Ana Somoza-Tornos and Mahinder Ramdin (TU Delft) for the fruitful discussions on CO_2RR; David Danaci (Imperial College London) for his guidance on the separation of C_2H_4/CO mixtures and his feedback on the manuscript; Marwan Sendi (Imperial College London) providing detailed insights into his solid-sorbent DAC process model; and the anonymous reviewers for their constructive suggestions on the manuscript.

Notes and references

1 International Energy Agency, *The Future of Petrochemicals towards More Sustainable Plastics and Fertilisers Together Secure Sustainable*, International Energy Agency technical report, 2018.
2 H. Zimmermann and R. Walzl, in *Ullmann's Encyclopedia of Industrial Chemistry*, ed. G. Bellussi, M. Bohnet, J. Bus, K. Drauz, H. Greim, K.-P. Jackel, U. Karst, A. Kleemann, G. Kreysa, T. Laird, W. Meier, E. Ottow, M. Roper, J. Scholtz, K. Sundmacher, R. Ulber and U. Wietelmann, Wiley, 7th edn, 2011, ch. Ethylene, vol. 40, pp. 1–58.
3 ExxonMobil, https://www.exxonmobil.co.uk/company/overview/uk-operations/fife-operations/our-operations.
4 Ineos, https://www.ineos.com/businesses/ineos-olefins-polymers-europe/products/.
5 SABIC UK, *Teesside – Wilton Site*, 2021.
6 Technical report prepared by the UK Department of Energy and Climate Change and Department for Business, Innovation and Skills, *Industrial Decarbonisation and Energy Efficiency Roadmaps to 2050 Chemicals*, 2015.
7 P. W. Griffin, G. P. Hammond and J. B. Norman, *Appl. Energy*, 2018, **227**, 587–602.
8 Department for Business, Energy & Industrial Strategy and National Statistics, *2019 UK Greenhouse Gas Emissions, Final Figures*, 2021.
9 Element Energy Ltd, *Deep-Decarbonisation Pathways for UK Industry*, Climate Change Committee technical report, 2020.
10 P. Gabrielli, M. Gazzani and M. Mazzotti, *Ind. Eng. Chem. Res.*, 2020, **59**, 7033–7045.
11 M. Yang, X. Tian and F. You, *Ind. Eng. Chem. Res.*, 2018, **57**, 5980–5998.
12 J. van Haveren, E. L. Scott and J. Sanders, *Biofuels, Bioprod. Biorefin.*, 2008, **2**, 41–57.
13 D. S. Mallapragada, Y. Dvorkin, M. A. Modestino, D. V. Esposito, W. A. Smith, B.-M. Hodge, M. P. Harold, V. M. Donnelly, A. Nuz, C. Bloomquist, K. Baker, L. C. Grabow, Y. Yan, N. N. Rajput, R. L. Hartman, E. J. Biddinger, E. S. Aydil and A. D. Taylor, *Joule*, 2023, **7**, 23–41.
14 A. Somoza-Tornos, O. J. Guerra, A. M. Crow, W. A. Smith and B.-M. Hodge, *iScience*, 2021, **24**, 102813.
15 M. Häußler, M. Eck, D. Rothauer and S. Mecking, *Nature*, 2021, **590**, 423–427.

16 O. Dogu, M. Pelucchi, R. Van de Vijver, P. H. Van Steenberge, D. R. D'hooge, A. Cuoci, M. Mehl, A. Frassoldati, T. Faravelli and K. M. Van Geem, *Prog. Energy Combust. Sci.*, 2021, **84**, 100901.
17 J.-P. Lange, *Energy Environ. Sci.*, 2021, **14**, 4358–4376.
18 BEIS, *Net Zero Strategy: Build Back Greener*, Department of Business, Energy and Industrial Strategy technical report, 2021.
19 SusChem, Cefic, PlasticsEurope, EuPC and ECP4, *Sustainable Plastics Strategy*, 2020.
20 Z. O. G. Schyns and M. P. Shaver, *Macromol. Rapid Commun.*, 2021, **42**, 2000415.
21 G. Lopez, M. Artetxe, M. Amutio, J. Bilbao and M. Olazar, *Renewable Sustainable Energy Rev.*, 2017, **73**, 346–368.
22 I. Vollmer, M. J. F. Jenks, M. C. P. Roelands, R. J. White, T. van Harmelen, P. de Wild, G. P. van der Laan, F. Meirer, J. T. F. Keurentjes and B. M. Weckhuysen, *Angew. Chem., Int. Ed.*, 2020, **59**, 15402–15423.
23 BEIS, *Carbon Capture, Usage and Storage*, Department of Business, Energy and Industrial Strategy technical report, 2022.
24 I. Esau and R. Watts, *Upstream*, 2021.
25 GE Gas Power, *Technip Energies and GE Gas Power Awarded FEED Study for Teesside Power, Carbon Capture and Compression Project in the UK*, 2021.
26 BP p.l.c, *BP Selects Johnson Matthey's LCH Technology for Its First Low Carbon (Blue) Hydrogen Project*, 2023.
27 HM Government, *CCUS Net Zero Investment Roadmap. Capturing Carbon and a Global Opportunity.*, 2023.
28 S. Deutz and A. Bardow, *Nat. Energy*, 2021, **6**, 203–213.
29 National Grid Electricity System Operator, *Historic Generation Mix & Carbon Intensity*, 2020.
30 A. Velazquez Abad and P. E. Dodds, *Energy Policy*, 2020, **138**, 111300.
31 A. H. Reksten, M. S. Thomassen, S. Møller-Holst and K. Sundseth, *Int. J. Hydrogen Energy*, 2022, **47**, 38106–38113.
32 C. Tsay, R. C. Pattison, M. R. Piana and M. Baldea, *Comput. Chem. Eng.*, 2018, **112**, 180–189.
33 C. F. Heuberger, I. Staffell, N. Shah and N. Mac Dowell, *Nat. Energy*, 2018, **3**, 634–640.
34 S. R. Nicholson, N. A. Rorrer, A. C. Carpenter and G. T. Beckham, *Joule*, 2021, **5**, 673–686.
35 T. Rommens, A. Tenhunen, L. Mortensen and I. Vanderreydt, *Greenhouse Gas Emissions and Natural Capital Implications of Plastics (Including Biobased Plastics)*, European Environment Agency – European Topic Centre on Waste and Materials in a Green Economy technical report, 2021.
36 P. De Luna, C. Hahn, D. Higgins, S. A. Jaffer, T. F. Jaramillo and E. H. Sargent, *Science*, 2019, **364**, eaav3506.
37 M. J. Orella, S. M. Brown, M. E. Leonard, Y. Román-Leshkov and F. R. Brushett, *Energy Technol.*, 2020, **8**, 1–12.
38 S. Verma, B. Kim, H.-R. M. Jhong, S. Ma and P. J. A. Kenis, *ChemSusChem*, 2016, **9**, 1972–1979.
39 M. Jouny, W. Luc and F. Jiao, *Ind. Eng. Chem. Res.*, 2018, **57**, 2165–2177.
40 M. A. Adnan and M. G. Kibria, *Appl. Energy*, 2020, **278**, 1–12.
41 H. Kim, B. Lee, D. Lim, C. Choe and H. Lim, *Green Chem.*, 2021, **23**, 7635–7645.
42 A. J. Welch, I. A. Digdaya, R. Kent, P. Ghougassian, H. A. Atwater and C. Xiang, *ACS Energy Lett.*, 2021, **6**, 1540–1549.
43 M. Moreno-Gonzalez, A. Berger, T. Borsboom-Hanson and W. Mérida, *Energy Convers. Manage.*, 2021, **244**, 1–17.
44 Z. Zhao, J. Jiang and F. Wang, *J. Energy Chem.*, 2021, **56**, 193–202.
45 T. N. Do, C. You and J. Kim, *Energy Environ. Sci.*, 2022, **15**, 169–184.
46 W. Hoppe, S. Bringezu and N. Wachter, *J. CO_2 Util.*, 2018, **27**, 170–178.
47 A. P. Ortiz-Espinoza, M. M. Noureldin, M. M. El-Halwagi and A. Jiménez-Gutiérrez, *Comput. Chem. Eng.*, 2017, **107**, 237–246.
48 M. Ramdin, B. De Mot, A. R. Morrison, T. Breugelmans, L. J. Van Den Broeke, J. P. Trusler, R. Kortlever, W. De Jong, O. A. Moultos, P. Xiao, P. A. Webley and T. J. Vlugt, *Ind. Eng. Chem. Res.*, 2021, **60**, 17862–17880.
49 I. Ioannou, S. C. D'Angelo, A. J. Martín, J. Pérez-Ramírez and G. Guillén-Gosálbez, *ChemSusChem*, 2020, **13**, 6370–6380.
50 L. Berkelaar, J. van der Linde, J. Peper, A. Rajhans, D. Tiemessen, L. van der Ham and H. van den Berg, *Chem. Eng. Res. Des.*, 2022, **182**, 194–206.
51 A. Kaetelhoen, R. Meys, S. Deutz, S. Suh and A. Bardow, *Proc. Natl. Acad. Sci. U. S. A.*, 2019, **166**, 11187–11194.
52 B. Fais, I. Keppo, M. Zeyringer, W. Usher and H. Daly, *Energy Strategy Rev.*, 2016, **13–14**, 154–168.
53 National Grid ESO, *Future Energy Scenarios 2022*, 2022.
54 HM Government, *Industrial Decarbonisation Strategy*, Department of Business, Energy and Industrial Strategy technical report, 2021.
55 M. Victoria, K. Zhu, T. Brown, G. B. Andresen and M. Greiner, *Nat. Commun.*, 2020, **11**, 6223.
56 M. Gazzani, D. M. Turi and G. Manzolini, *Int. J. Greenhouse Gas Control*, 2014, **20**, 293–309.
57 Y. Liu, H. Kamata, H. Ohara, Y. Izumi, D. S. W. Ong, J. Chang, C. K. Poh, L. Chen and A. Borgna, *Ind. Eng. Chem. Res.*, 2020, **59**, 8728–8739.
58 G. Towler and R. Sinnot, *Chemical Engineering Design – Principles, Practice and Economics of Plant and Process Design*, Elsevier, 3rd edn, 2022.
59 S. Jenkins, *Chemical Engineering Plant Cost Index: 2019 Annual Value*, 2019.
60 S. Hernandez-Aldave and E. Andreoli, *Catalysts*, 2020, **10**(6), 713.
61 J. Na, B. Seo, J. Kim, C. W. Lee, H. Lee, Y. J. Hwang, B. K. Min, D. K. Lee, H.-S. Oh and U. Lee, *Nat. Commun.*, 2019, **10**, 5193.
62 T. Wang, X. Cao and L. Jiao, *Angew. Chem., Int. Ed.*, 2022, **61**, e202213328.
63 M. Duarte, J. Hereijgers, N. Daems, S. Van Daele and T. Breugelmans, *J. Environ. Chem. Eng.*, 2022, **10**, 107836.

64 Q. Xu, A. Xu, S. Garg, A. B. Moss, I. Chorkendorff, T. Bligaard and B. Seger, *Angew. Chem., Int. Ed.*, 2023, **62**, e202214383.
65 T. Alerte, J. P. Edwards, C. M. Gabardo, C. P. OBrien, A. Gaona, J. Wicks, A. Obradović, A. Sarkar, S. A. Jaffer, H. L. MacLean, D. Sinton and E. H. Sargent, *ACS Energy Lett.*, 2021, **6**, 4405–4412.
66 B. Endrődi, E. Kecsenovity, A. Samu, F. Darvas, R. V. Jones, V. Török, A. Danyi and C. Janáky, *ACS Energy Lett.*, 2019, **4**, 1770–1777.
67 J. A. Rabinowitz and M. W. Kanan, *Nat. Commun.*, 2020, **11**, 5231.
68 P. Mardle, S. Cassegrain, F. Habibzadeh, Z. Shi and S. Holdcroft, *J. Phys. Chem. C*, 2021, **125**, 25446–25454.
69 C. Wang, Y. Liu, H. Ren, Q. Guan, S. Chou and W. Li, *ACS Catal.*, 2022, **12**, 2513–2521.
70 X. Y. Zhang, W. J. Li, X. F. Wu, Y. W. Liu, J. Chen, M. Zhu, H. Y. Yuan, S. Dai, H. F. Wang, Z. Jiang, P. F. Liu and H. G. Yang, *Energy Environ. Sci.*, 2022, **15**, 234–243.
71 Y. Ji, C. Yang, L. Qian, L. Zhang and G. Zheng, *J. Colloid Interface Sci.*, 2021, **600**, 847–853.
72 C.-T. Dinh, T. Burdyny, M. G. Kibria, A. Seifitokaldani, C. M. Gabardo, F. Pelayo García De Arquer, A. Kiani, J. P. Edwards, P. De Luna, O. S. Bushuyev, C. Zou, R. Quintero-Bermudez, Y. Pang, D. Sinton and E. H. Sargent, *Science*, 2018, **360**, 783–787.
73 A. Gawel, T. Jaster, D. Siegmund, J. Holzmann, H. Lohmann, E. Klemm and U.-P. Apfel, *iScience*, 2022, **25**, 104011.
74 *Green Hydrogen Cost Reduction. Scaling up Electrolysers to Meet the 1.5 C Climate Goal*, International Renewable Energy Agency technical report, 2020.
75 BEIS, *Hydrogen Production Costs 2021*, Department of Business, Energy and Industrial Strategy technical report, 2021.
76 A. Mayyas, M. Ruth, B. Pivovar, G. Bender and K. Wipke, *Manufacturing Cost Analysis for Proton Exchange Membrane Water Electrolyzers*, NREL technical report, 2018.
77 J. E. Bachman, D. A. Reed, M. T. Kapelewski, G. Chachra, D. Jonnavittula, G. Radaelli and J. R. Long, *Energy Environ. Sci.*, 2018, **11**, 2423–2431.
78 D. A. Jones, *Technoeconomic Evaluation of MEA versus Mixed Amines and a Catalyst System for CO2 Removal at Near-Commercial Scale at Duke Energy Gibson 3 Plant and Duke Energy Buck NGCC Plant*, Lawrence Livermore National Laboratory technical report, 2018.
79 G. A. Buchner, A. W. Zimmermann, A. E. Hohgräve and R. Schomäcker, *Ind. Eng. Chem. Res.*, 2018, **57**, 8502–8517.
80 A. Hauch, R. Küngas, P. Blennow, A. B. Hansen, J. B. Hansen, B. V. Mathiesen and M. B. Mogensen, *Science*, 2020, **370**, eaba6118.
81 R. Küngas, *J. Electrochem. Soc.*, 2020, **167**, 044508.
82 C. Mittal, C. Hadsbjerg and P. Blennow, *Chem. Eng. World*, 2017, **52**, 44–46.
83 N. B. Jakobsson, C. F. Pedersen and J. B. Hansen, *Process for Producing CO from CO_2 in a Solid Oxide Electrolysis Cell, Haldor Topsoe A/S, US Pat., US 10494728 B2, 2019.*
84 G. Glenk, P. Holler and S. Reichelstein, *Energy Environ. Sci.*, 2023, **16**, 6058–6070.
85 H. Böhm, A. Zauner, D. C. Rosenfeld and R. Tichler, *Appl. Energy*, 2020, **264**, 114780.
86 Clean Hydrogen Joint Undertaking, *Strategic Research and Innovation Agenda 2021–2027*, 2022.
87 O. Schmidt, A. Hawkes, A. Gambhir and I. Staffell, *Nat. Energy*, 2017, **2**, 17110.
88 H. Nami, O. B. Rizvandi, C. Chatzichristodoulou, P. V. Hendriksen and H. L. Frandsen, *Energy Convers. Manage.*, 2022, **269**, 116162.
89 O. Schmidt, A. Gambhir, I. Staffell, A. Hawkes, J. Nelson and S. Few, *Int. J. Hydrogen Energy*, 2017, **42**, 30470–30492.
90 T. Smolinka, N. Wiebe, P. Sterchele, A. Palzer, F. Lehner, M. Jansen, S. Kiemel, R. Miehe, S. Wahren and F. Zimmermann, *Studie IndWEDe. Industrialisierung Der Wasserelektrolyse in Deutschland: Chancen Und Herausforderungen Für Nachhaltigen Wasserstoff Für Verkehr, Strom Und Wärme*, Bundesministerium für Verkehr und digitale Infrastruktur (BMVI) technical report, 2018.
91 Environment Agency, *Wilton Olefins Installation. Permit Number EPR/BS3590IE*, Environment Agency technical report, 2016.
92 R. Chauvy, D. Verdonck, L. Dubois, D. Thomas and G. De Weireld, *J. CO_2 Util.*, 2021, **47**, 1–10.
93 M. Pérez-Fortes, J. C. Schöneberger, A. Boulamanti and E. Tzimas, *Appl. Energy*, 2016, **161**, 718–732.
94 J. Price, I. Keppo and P. E. Dodds, *Energy*, 2023, **262**, 125450.
95 J. D. Williams, J. Williamson, D. Parkes, D. J. Evans, K. L. Kirk, N. Sunny, E. Hough, H. Vosper and M. C. Akhurst, *J. Energy Storage*, 2022, **53**, 105109.
96 East Coast Hydrogen, *East Coast Hydrogen Feasibility Report*, 2021.
97 T. Terlouw, C. Bauer, R. McKenna and M. Mazzotti, *Energy Environ. Sci.*, 2022, **15**, 3583–3602.
98 D. S. Mallapragada, E. Gençer, P. Insinger, D. W. Keith and F. M. O'Sullivan, *Cell Rep. Phys. Sci.*, 2020, **1**, 100174.
99 M. Sendi, M. Bui, N. Mac Dowell and P. Fennell, *One Earth*, 2022, **5**, 1153–1164.
100 IEAGHG, *Deployment of CCS in the Cement Industry*, 2013.
101 S. Hughes and A. Zoelle, *Cost of Capturing CO_2 from Industrial Sources*, National Energy Technology Laboratory technical report, 2022.
102 BEIS, *Valuation of Greenhouse Gas Emissions: For Policy Appraisal and Evaluation*, 2020.
103 United Utilities, *Wholesale Sewerage*, United Utilities technical report, 2019.
104 ICIS, *ICIS Chemical Business*, ICIS technical report, 2019.
105 M. Rivarolo, D. Bellotti, A. Mendieta and A. Massardo, *Energy Convers. Manage.*, 2014, **79**, 74–84.
106 J. G. Speight, *Rules of Thumb for Petroleum Engineers*, John Wiley & Sons, 2017.
107 R. Wiser, J. Rand, J. Seel, P. Beiter, E. Baker, E. Lantz and P. Gilman, *Nat. Energy*, 2021, **6**, 555–565.

108 F. Keller, R. P. Lee and B. Meyer, *J. Cleaner Prod.*, 2020, **250**, 119484.
109 M. Hurley, *European Ethylene Contract Reference Price in April Set at 1665 €/t for April, ICIS News*, 2022.
110 C. M. Gabardo, C. P. O'Brien, J. P. Edwards, C. McCallum, Y. Xu, C. T. Dinh, J. Li, E. H. Sargent and D. Sinton, *Joule*, 2019, **3**, 2777–2791.
111 P. Jeanty, C. Scherer, E. Magori, K. Wiesner-Fleischer, O. Hinrichsen and M. Fleischer, *J. CO_2 Util.*, 2018, **24**, 454–462.
112 M. Goldman, A. Prajapati, E. Duoss, S. Baker and C. Hahn, *Curr. Opin. Electrochem.*, 2023, **39**, 101248.
113 G. Leonzio, B. Chachuat and N. Shah, *Sustain. Prod. Consum.*, 2023, **43**, 124–139.
114 F. Li, A. Thevenon, A. Rosas-Hernández, Z. Wang, Y. Li, C. M. Gabardo, A. Ozden, C. T. Dinh, J. Li, Y. Wang, J. P. Edwards, Y. Xu, C. McCallum, L. Tao, Z. Q. Liang, M. Luo, X. Wang, H. Li, C. P. O'Brien, C. S. Tan, D. H. Nam, R. Quintero-Bermudez, T. T. Zhuang, Y. C. Li, Z. Han, R. D. Britt, D. Sinton, T. Agapie, J. C. Peters and E. H. Sargent, *Nature*, 2019, **577**, 509–513.
115 M. Zhong, K. Tran, Y. Min, C. Wang, Z. Wang, C.-T. Dinh, P. De Luna, Z. Yu, A. S. Rasouli, P. Brodersen, S. Sun, O. Voznyy, C.-S. Tan, M. Askerka, F. Che, M. Liu, A. Seifitokaldani, Y. Pang, S.-C. Lo, A. Ip, Z. Ulissi and E. H. Sargent, *Nature*, 2020, **581**, 178–183.
116 *ICIS News*, 2022.
117 T. Kato, M. Kubota, N. Kobayashi and Y. Suzuoki, *Energy*, 2005, **30**, 2580–2595.
118 H. Mohammadpour, R. Cord-Ruwisch, A. Pivrikas and G. Ho, *Chem. Eng. Sci.*, 2021, **246**, 117008.
119 A. Torchia and R. Shamseddine, *Saudi's SABIC Signs Deal to Use U.S. Shale Gas at British Plant*, 2015.
120 INEOS Group, *INEOS Insight Docks at Grangemouth Bringing US Shale Gas to the UK for the First Time*, 2016.
121 H. Ritchie, M. Roser and P. Rosado, Our World in Data, *Energy*, 2023, **https://ourworldindata.org/energy**.
122 D. J. C. MacKay, *Sustainable Energy–Without the Hot Air*, 2009.
123 G. L. Authority, *Land Area and Population Density, Ward and Borough*, 2018.
124 A. Kadak, *The Chemical Engineer*, 2022, June 972, **https://www.thechemicalengineer.com/features/energy-bringing-nuclear-back/**.
125 D. G. Caglayan, N. Weber, H. U. Heinrichs, J. Linßen, M. Robinius, P. A. Kukla and D. Stolten, *Int. J. Hydrogen Energy*, 2020, **45**, 6793–6805.
126 K. Allen, G. Baida, B. Balboa, L. Berton, B. Mk, B. Brooks, F. Dobashi, K. Hays, *et al.*, *Global Petrochemical Outlook H2 2019, Petrochemicals Special Report*, S&P Global Platts technical report, 2019.
127 X. Kan, L. Reichenberg, F. Hedenus and D. Daniels, *arXiv*, 2022, preprint, arXiv.2202.02257, DOI: **10.48550/arXiv.2202.02257**.
128 D. Freire Ordóñez, C. Ganzer, T. Halfdanarson, A. González Garay, P. Patrizio, A. Bardow, G. Guillén-Gosálbez, N. Shah and N. Mac Dowell, *Energy Adv.*, 2023, **2**, 2042–2054.
129 R. Taylor, E. Raphael, C. Lewis, R. Berridge and J. Howes, *Expansion of Hydrogen Production Pathways Analysis – Import Chains*, Department of Business, Energy & Industrial Strategy technical report, 2022.
130 Royal HaskoningDHV, *Norfolk Boreas, Greenhouse Gas Footprint Assessment*, ExA.AS-3.D14.V1, 2020.
131 S. E. Tanzer and A. Ramírez, *Energy Environ. Sci.*, 2019, **12**, 1210–1218.
132 Carbon Recycling International, *The Shunli CO_2-to-Methanol Plant: Commercial Scale Production in China*.
133 M. J. Matzen, M. H. Alhajji and Y. Demirel, *J. Adv. Chem. Eng.*, 2015, **5**, 1–13.
134 I. L. Wiesberg, J. L. de Medeiros, R. M. Alves, P. L. Coutinho and O. Q. Araújo, *Energy Convers. Manage.*, 2016, **125**, 320–335.
135 J. Albo, M. Alvarez-Guerra, P. Castaño and A. Irabien, *Green Chem.*, 2015, **17**, 2304–2324.
136 H. Yang, Y. Wu, G. Li, Q. Lin, Q. Hu, Q. Zhang, J. Liu and C. He, *J. Am. Chem. Soc.*, 2019, **141**, 12717–12723.
137 D. Yang, Q. Zhu, C. Chen, H. Liu, Z. Liu, Z. Zhao, X. Zhang, S. Liu and B. Han, *Nat. Commun.*, 2019, **10**, 1–9.
138 A. P. Periasamy, R. Ravindranath, S. M. Senthil Kumar, W. P. Wu, T. R. Jian and H. T. Chang, *Nanoscale*, 2018, **10**, 11869–11880.
139 L. Lu, X. Sun, J. Ma, D. Yang, H. Wu, B. Zhang, J. Zhang and B. Han, *Angew. Chem., Int. Ed.*, 2018, **130**, 14345–14349.
140 J. Albo, A. Sáez, J. Solla-Gullón, V. Montiel and A. Irabien, *Appl. Catal., B*, 2015, **176–177**, 709–717.
141 M. Ye, H. Li, Y. Zhao, T. Zhang and Z. Liu, in *Mesoscale Modeling in Chemical Engineering Part II*, ed. G. B. Marin and J. Li, Academic Press, 2015, ch. 5, vol. 47 of Advances in Chemical Engineering, pp. 279–335.
142 F. J. Keil, *Microporous Mesoporous Mater.*, 1999, **29**, 49–66.
143 Y. H. Chen, W. Hsieh, H. Chang and C. D. Ho, *J. Taiwan Inst. Chem. Eng.*, 2022, **130**, 103893.
144 S. Jasper and M. M. El-Halwagi, *Processes*, 2015, **3**, 684–698.
145 S. Rönsch, J. Schneider, S. Matthischke, M. Schlüter, M. Götz, J. Lefebvre, P. Prabhakaran and S. Bajohr, *Fuel*, 2016, **166**, 276–296.
146 G. Iaquaniello, S. Setini, A. Salladini and M. De Falco, *Int. J. Hydrogen Energy*, 2018, **43**, 17069–17081.
147 B. Li, L. Liu, M. Yue, Q. Niu, M. Li, T. Zhang, W. Xie and Q. Wang, *Green Chem.*, 2024, **26**, 103–121.
148 H. Pan and C. J. Barile, *Energy Environ. Sci.*, 2020, **13**, 3567–3578.
149 J. Liu, J. Yue, M. Lv, F. Wang, Y. Cui, Z. Zhang and G. Xu, *Carbon Resour. Convers.*, 2022, **5**, 1–14.
150 V. Spallina, I. C. Velarde, J. A. M. Jimenez, H. R. Godini, F. Gallucci and M. Van Sint Annaland, *Energy Convers. Manage.*, 2017, **154**, 244–261.
151 L. S. Layritz, I. Dolganova, M. Finkbeiner, G. Luderer, A. T. Penteado, F. Ueckerdt and J. U. Repke, *Appl. Energy*, 2021, **296**, 117049.
152 H. Yang, Q. Lin, Y. Wu, G. Li, Q. Hu, X. Chai, X. Ren, Q. Zhang, J. Liu and C. He, *Nano Energy*, 2020, **70**, 104454.

153 K. Liu, J. Wang, M. Shi, J. Yan, Q. Jiang, K. H. Liu, M. M. Shi, J. M. Yan, Q. Jiang and J. Z. Wang, *Adv. Energy Mater.*, 2019, **9**, 1900276.
154 H. B. Yang, S. F. Hung, S. Liu, K. Yuan, S. Miao, L. Zhang, X. Huang, H. Y. Wang, W. Cai, R. Chen, J. Gao, X. Yang, W. Chen, Y. Huang, H. M. Chen, C. M. Li, T. Zhang and B. Liu, *Nat. Energy*, 2018, **3**, 140–147.
155 Q. Lu, J. Rosen, Y. Zhou, G. S. Hutchings, Y. C. Kimmel, J. G. Chen and F. Jiao, *Nat. Commun.*, 2014, **5**, 1–6.
156 Y. Chen, C. W. Li and M. W. Kanan, *J. Am. Chem. Soc.*, 2012, **134**, 19969–19972.
157 S. Verma, Y. Hamasaki, C. Kim, W. Huang, S. Lu, H. R. M. Jhong, A. A. Gewirth, T. Fujigaya, N. Nakashima and P. J. Kenis, *ACS Energy Lett.*, 2018, **3**, 193–198.
158 Haldor Topsoe, **https://www.topsoe.com/processes/carbon-monoxide**.
159 Y. Song, Z. Zhou, X. Zhang, Y. Zhou, H. Gong, H. Lv, Q. Liu, G. Wang and X. Bao, *J. Mater. Chem. A*, 2018, **6**, 13661–13667.
160 A. Hauch, K. Brodersen, M. Chen, C. Graves, S. H. Jensen, P. S. Jørgensen, P. V. Hendriksen, M. B. Mogensen, S. Ovtar and X. Sun, *ECS Trans.*, 2017, **75**, 3.
161 A. Nechache and S. Hody, *Renewable Sustainable Energy Rev.*, 2021, **149**, 111322.
162 Y. Ni, Y. Liu, Z. Chen, M. Yang, H. Liu, Y. He, Y. Fu, W. Zhu and Z. Liu, *ACS Catal.*, 2019, **9**, 1026–1032.
163 F. Jiao, J. Li, X. Pan, J. Xiao, H. Li, H. Ma, M. Wei, Y. Pan, Z. Zhou, M. Li, S. Miao, J. Li, Y. Zhu, D. Xiao, T. He, J. Yang, F. Qi, Q. Fu and X. Bao, *Science*, 2016, **351**, 1065–1068.
164 D. Xiang, S. Yang and Y. Qian, *Energy Convers. Manage.*, 2016, **110**, 33–41.
165 H. P. Duong, N.-H. Tran, G. Rousse, S. Zanna, M. W. Schreiber and M. Fontecave, *ACS Catal.*, 2022, **12**, 10285–10293.
166 K. J. P. Schouten, Z. Qin, E. P. Gallent and M. T. Koper, *J. Am. Chem. Soc.*, 2012, **134**, 9864–9867.
167 N. S. Romero Cuellar, C. Scherer, B. Kaçkar, W. Eisenreich, C. Huber, K. Wiesner-Fleischer, M. Fleischer and O. Hinrichsen, *J. CO_2 Util.*, 2020, **36**, 263–275.
168 G. Centi, A. Quadrelli and S. Perathoner, *Energy Environ. Sci.*, 2013, **6**, 1711–1731.
169 J. Gao, C. Jia and B. Liu, *Catal. Sci. Technol.*, 2017, **7**, 5602–5607.
170 M. A. Marvast, M. Sohrabi, S. Zarrinpashne and G. Baghmisheh, *Chem. Eng. Technol.*, 2005, **28**, 78–86.
171 S. Najari, G. Gróf, S. Saeidi and F. Gallucci, *Int. J. Hydrogen Energy*, 2019, **44**, 4630–4649.
172 T. N. Do and J. Kim, *Energy Convers. Manage.*, 2020, **214**, 112866.
173 H. Q. Liang, S. Zhao, X. M. Hu, M. Ceccato, T. Skrydstrup and K. Daasbjerg, *ACS Catal.*, 2021, **11**, 958–966.